Master's thesis

NTNU
Norwegian University of Science and Technology
Faculty of Engineering
Department of Structural Engineering

Martin Nikolai Kanestrøm
Robin Bekkos

Tensile capacity of hollow core slabs subjected to concentrated edge loads

Master's thesis in Civil and Environmental Engineering
Supervisor: Prof. Terje Kanstad
Co-supervisor: Leidulv Vinje

June 2021

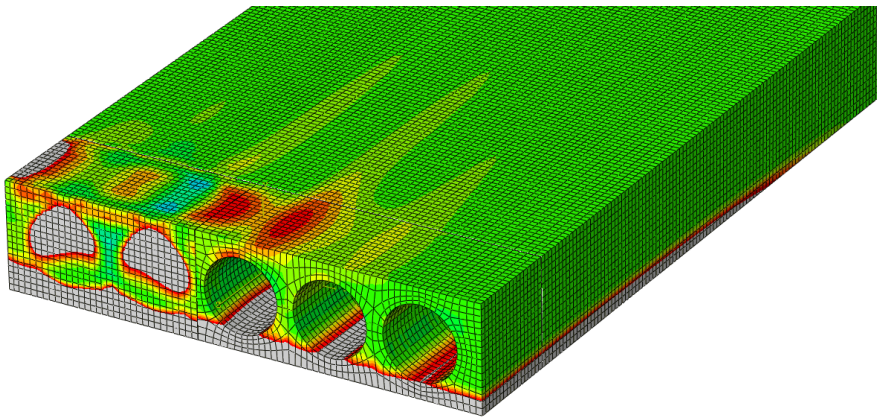

NTNU
Norwegian University of
Science and Technology

Martin Nikolai Kanestrøm
Robin Bekkos

Tensile capacity of hollow core slabs subjected to concentrated edge loads

Master's thesis in Civil and Environmental Engineering
Supervisor: Prof. Terje Kanstad
Co-supervisor: Leidulv Vinje
June 2021

Norwegian University of Science and Technology
Faculty of Engineering
Department of Structural Engineering

NTNU
Norwegian University of
Science and Technology

Department of Structural Engineering
Faculty of Engineering
NTNU – Norwegian University of Science and Technology

ACCESSIBILITY

OPEN

MASTER THESIS 2021

SUBJECT AREA:	DATE:	NO. OF PAGES:
CONCRETE STRUCTURES	June 10, 2021	65 (thesis) + 6 (Appendix)

TITLE:

Tensile capacity of hollow core slabs subjected to concentrated edge loads

Strekkapasitet av hulldekker påført konsentrerte punktlaster på kanten av dekket

BY:

Robin Bekkos

Martin Nikolai Kanestrøm

SUMMARY:
Hollow core slabs subjected to concentrated edge loads from balcony connections have their first voids cast with concrete to install the connection details and increase the capacity of the slab. Some slabs experience cracks in the top flange over the unfilled void behind the concentrated edge load due to high tensile stresses. Because the hollow core slabs usually contain reinforcement only in the longitudinal direction, the tensile capacity in the transverse direction depends solely on the concrete´s tensile strength. Further, it is specified in the hollow core standard NS-EN 1168 that the hollow core slabs can be expected to distribute the concentrated load to the rest of the slab system, reducing the stresses on the loaded slab.

The load distribution and tensile stress analysis were done using, Abaqus/CAE. First, the theory of load distribution in a system of hollow core slabs was analyzed. Then a local tensile stress analysis was done with three different slab types by varying the load placement. The highest principal tensile stresses were obtained by varying the vertical and horizontal load, the placement of the connection, the amount of prestressed reinforcement, the mesh size, and the connection plate placement. The capacity for punching shear was calculated and compared to results from the analysis.

The 200mm HCS experiences tensile stresses higher than the tensile strength of the concrete for all the loads. The 265mm and 320mm HCS experience lower stresses than the 200mm HCS, but some are close to the tensile strength. The worst tensile stresses act when the all the slabs are loaded close to the supports. The eccentricity moment transferred to the HCS from the balcony influences the tensile stresses. However, in reality, they are often not transferred to the slab due to the connection detail. Other parameters such as placement of the steel plate, amount of prestressed reinforcement, and the horizontal load have little influence. Results show that the tensile stresses are mainly affected by the size and placement of the vertical load and can cause cracks and failure in the loaded slab.

RESPONSIBLE TEACHER: Prof. Terje Kanstad

SUPERVISOR(S): Prof. Terje Kanstad, Prof. Leidulv Vinje

CARRIED OUT AT: Department of structural engineering

Abstract

Hollow core slabs subjected to concentrated edge loads from balcony connections have their first voids cast with concrete to install the connection details and increase the capacity of the slab. Some slabs experience cracks in the top flange over the unfilled void behind the concentrated edge load due to high tensile stresses. Because the hollow core slabs usually contain reinforcement only in the longitudinal direction, the tensile capacity in the transverse direction depends solely on the concrete´s tensile strength. Further, it is specified in the hollow core standard NS-EN 1168 that the hollow core slabs can be expected to distribute the concentrated load to the rest of the slab system, reducing the stresses on the loaded slab.

The load distribution and tensile stress analysis were done using a finite element analysis tool, Abaqus/CAE. First, the theory of load distribution in a system of hollow core slabs was analyzed, then the results were applied to a single hollow core slab under a concentrated load. The load applied was equal to the weight of either of the two chosen balconies and their respective live loads. The local tensile stress analysis was done with three different slab types with heights of 200mm, 265mm, and 320mm, and the loads were placed in the center of the span, 1000mm from the support and at both places simultaneously. The highest principal tensile stresses were obtained for the three slab types by varying the vertical and horizontal load, the placement of the connection, the amount of prestressed reinforcement, the mesh size, and the connection plate placement. The capacity for punching shear was calculated and compared to results from the analysis.

The 200mm HCS experiences tensile stresses higher than the tensile strength of the concrete for all the loads presented and should therefore be designed with caution. The 265mm and 320mm HCS experience lower stresses than the 200mm HCS, but some are close to the tensile strength. For all the slabs, regardless of the height, the worst tensile stresses act when the slabs are loaded close to the supports. The eccentricity moment transferred to the HCS from the balcony influences the tensile stresses. However, in reality, they are often not transferred to the hollow core slab due to the connection detail. Other parameters such as placement of the steel plate, amount of prestressed reinforcement, and the horizontal load in the connection have little influence. Results show that the tensile stresses are mainly affected by the size and placement of the vertical load and can cause cracks and failure in the loaded slab.

Sammendrag

Hulldekker benyttes ofte i prosjekter hvor det skal konstrueres balkonger slik at disse må festes inn i sidekant på dekkene. For å øke kapasiteten og installere forbindelsen støpes de to første hullene i hulldekkene med betong. Den resulterende punktlastoverføringen fra balkongen kan føre til at det belastede hulldekket sprekker opp i et område bak lastpåføringen, fordi strekkspenningene i betongen blir for store. Forspente hulldekker armeres kun i lengderetning, noe som gjør at kapasiteten for strekk i tverretningen begrenses av betongens strekkfasthet. Videre er det spesifisert i hulldekkestandarden, NS-EN 1168, at det belastede hulldekket fordeler punktlasten til hulldekkene bak, noe som resulterer i lavere spenninger i det belastede dekket.

Analyser av lastfordelingen og strekkspenningene i den belastede platen var gjort med det numeriske elementmetodeprogrammet, Abaqus/CAE. Først ble lastfordelingsantagelsen undersøkt. Deretter ble resultatene fra denne analysen benyttet i en analyse av ett hulldekke påført en konsentrert endelast fra to ulike balkonger og deres respektive nyttelast. Analysene ble gjort for tre ulike hulldekker, HD200, HD265 og HD320, og lastene ble påført i midten av spennet, 1000mm fra opplegget og ved begge plasseringer samtidig. Spenningsoppførselen lokalt i hulldekket ble analysert, og systemets oppførsel under lastfordelingen ble påsatt som en last langs fugen mot det neste dekket i systemet. Hovedspenningene som ga mest strekk i overkant av hullet bak den påførte lasten ble funnet for de tre ulike dekkene, ved å variere den påførte vertikale og horisontale konsentrerte lasten, plasseringen av lasten, mengden forspent armering, størrelsen på meshet og plasseringen av stålplaten i underkant av den påførte lasten.

HD200 opplevde strekkspenninger større enn strekkfastheten for betong for alle lasttilfeller den ble utsatt for, og bør derfor bli brukt med varsomhet. HD265 og HD320 opplevde mindre spenninger, men for noen lasttilfeller var strekkspenningene nær strekkfastheten. De største strekkspenningene, uavhengig av dekkehøyden, opptrer når dekkene er belastet nært opplegget. Eksentristetsmoment, overført til hulldekket ved balkongopplegget på grunn av en åpning mellom balkong og hulldekket (figur: 17 og 18), har en stor påvirkning på de opptredende strekkspenningene. I virkeligheten overføres ikke momentet så ofte på grunn av detailene i balkongforbindelsen. Andre parametere som plasseringen av stålplaten, mengden forspent armering og variasjon i horisontallast fra balkongen har liten innvirkning på strekkspenningene. Resultatene viser at strekkspenningene i hovedsak blir større på grunn av økt vertikal last, samt plasseringen av lasten på hulldekket, noe som kan føre til sprekker og brudd i betongen.

Preface

This Master thesis with the Concrete structures specialization was performed at the department of structural engineering at NTNU in the study program for Civil and Environmental engineering at NTNU. The thesis is listed as a subject with 30 credits under the subject code TKT4950.

The process of writing this thesis have been a long and educational experience. We have experienced that small problems often require the longest time to solve. During the 20 weeks, we had a lot of fun together, and always kept a smile on our faces.

We would like to thank our supervisor at NTNU, prof. Terje Kanstad for the continuous support, insight, broad competence and for always leaving the door open. We would also like to thank our external supervisor, prof. Leidulv Vinje, for presenting us with this problem, his availability, broad knowledge, and good discussions. His presence helped us to narrow down and solve the problems along the way.

Additionally, we would like to thank both Øystein Rønningen from Spenncon and Arvid Loe from Invisible Connections for answering important questions and providing necessary information.

Contents

Abstract ii

Sammendrag iii

Preface iv

Table of contents viii

1 Introduction 1

1.1 Motivation . . . 1

1.2 Scope and Limitation . . . 1

2 Theory 3

2.1 Elements and materials . . . 3

2.2 General behavior of hollow core slabs . . . 4

2.3 Load distribution between hollow core slabs . . . 5

2.4 Shear . . . 8

2.4.1 Web shear strength . . . 11

2.5 Torsion . . . 11

2.6 Shear and torsion interaction . . . 12

2.7 Non-rigid supports . . . 13

2.8 Edge anchorage . . . 13

2.9 Principal stresses . . . 14

2.10 Previous research . . . 15

3 Methodology 16

3.1 Load distribution model . . . 16

3.2 Local failure model . . . 17

3.2.1 Parameter variation . . . 20

3.2.2 Loads applied to the model 22
3.2.2.1 Vertical forces from the balconies 23
3.2.2.2 Horizontal forces from the balconies 23
3.2.2.3 Loads from the prestressed reinforcement 25
3.2.2.4 Shear forces due to system behavior 25
3.2.2.5 Moment due to connection detail 26

4 Finite element modeling **28**

4.1 Software 28
4.1.1 Modeling approach 28
4.2 Load distribution model 30
4.2.1 Hollow core system 30
4.2.2 Materials and orientations 31
4.2.3 Boundary conditions and load 32
4.2.4 Interactions 33
4.2.5 Partitioning and mesh 33
4.3 Local failure model 34
4.3.1 Materials 35
4.3.2 Constraints and boundary conditions 35
4.3.3 Partitioning and mesh 35
4.3.4 Loads applied to the model 36
4.3.4.1 Vertical load 37
4.3.4.2 Horizontal load 39
4.3.4.3 Eccentricity moment 39
4.3.4.4 Prestressed reinforcement 40
4.3.4.5 Traction forces from load distribution 40
4.3.4.6 Total load situation 41

5 Results **42**

5.1 Load distribution model 42

5.1.1 Diagrams from Abaqus/CAE 42

5.1.2 Load distribution factors 43

5.1.3 Shear forces 44

5.1.4 Reaction forces and concentrated forces in the corners 45

5.2 Local failure model 46

5.2.1 Principal stresses 48

5.2.2 Variation in the number of reinforcement bars 51

5.2.3 Effect of two loads on one hollow core slab 52

5.2.4 Steel plate placement 52

5.2.5 Numerical errors 53

6 Capacity control **54**

7 Discussion **55**

7.1 Load distribution model 55

7.2 Local failure model 56

7.2.1 Balcony size 56

7.2.2 Vertical load 56

7.2.3 Horizontal load 57

7.2.4 Effect of prestressing and variation in number of tendons 57

7.2.5 Eccentricity moment & connection detail 58

7.2.6 Effect of one vs. two balcony connections on one hollow core slab 59

7.2.7 Placement of the steel plate 59

7.2.8 Capacity control of punching shear and the use of different types of HCS . 59

7.2.9 Sources of error 60

8 Conclusion and future work **62**

8.1 Conclusion 62

8.2 Future work 63

Bibliography **64**

Appendix **66**

A Transfer of prestress 66

B Prestress information 67

C Examples of possible solutions 67

D Loads applied the finite element model 69

D.1 Traction loads for center loaded slabs 69

D.2 Traction loads for slabs loaded 1000mm from the support's end 70

1 Introduction

1.1 Motivation

Hollow core slabs are widely used in construction today as precast solutions. These units have several advantages that make them dependable and popular in the building industry. Precast elements can reduce material costs from concrete, steel reinforcement, and the labor of casting the concrete, therefore being advantageous for the economy. These units are factory-made, and production involves a moving mold that extrudes wet concrete over already prestressed steel cables. After the concrete has hardened, units are cut into the required length. There is only reinforcement in the longitudinal direction, meaning along the length of the slab, so in the transverse direction, meaning along the width of the slab, the tensile strength depends solely on the tensile strength of the concrete. The use of prestressed steel strands in these units allows for constructing large spans, e.g., floors.

Hollow core slabs, further abbreviated as HCS subjected to concentrated edge load, are not widely researched. However, it is observed that some slabs experience cracks in the top flange behind the load due to high tensile stresses caused by balcony connections. These local tensile stresses are essential to control as they can lead to failure in the HCS. By understanding and varying the loads affecting these stresses, the problem can be enlightened. As the construction industry tends to be more and more interested in using prefabricated elements in new structures, prestressed precast HCS is a desirable topic today. Additionally, the motivation to learn a complicated FEA tool is present, so using Abaqus/CAE to analyze the problem by accurately modeling the behavior is very convenient, for that matter. The use of Abaqus/CAE also helps increase the understanding of the finite element method.

1.2 Scope and Limitation

The scope for this master thesis is to look at whether concentrated edge loads on a hollow core slab are a problem or not due to the resulting tensile stresses that occur behind the applied load. In order to study whether these concentrated edge loads represent a problem, this thesis will examine factors that may contribute to increased tensile stresses in the slabs. Different HCS will be analyzed with multiple varying load conditions. Parameters such as the number of reinforcement bars, depth of the load-distributing steel plate are varied. Additionally, the effect of two loads applied to a single slab and numerical errors of the results are obtained. Due to the observed cracks, there is a desire to do a more thorough analysis to clarify if concentrated edge loads are a problem within the precast elements due to the arising tensile stresses.

A second scope for this thesis is to do further analysis on the load distribution between the HCS. Today's regulations for load distribution in a hollow core slab system exposed to concentrated

loading are based on research done in the 1980s. The system will distribute the concentrated load within the system, reducing the stresses acting on a single slab. This condition is a topic of interest when researching the tensile stresses in the top flange of the slab.

The focus will be finite element modeling of a floor system with concentrated edge loads to analyze the behavior. First, it is of interest to verify the load distribution model based on theory of elasticity, using Abaqus/CAE. After the load distribution is analyzed, the behavior of the slabs behind the loaded slab is applied to the longitudinal edge of a single hollow core slab. The single slab is analyzed by checking the tensile stresses over the void behind the load. These two models will be used to understand the current regulations and examine the possibility of high tensile stresses in the slab to prevent cracks and damage to structures. In order to fulfill these tasks, this thesis will provide the necessary background theory and regulations used today. Finite element models in Abaqus/CAE will be made, explained, and used to present the results and discussion.

2 Theory

2.1 Elements and materials

Hollow core elements are produced with a standard element width of 1200mm. The height varies depending on the element type. The concrete most often used, in hollow core elements, are of quality C45. Material characteristics for the specific concrete quality is found in NS-EN 1992-1-1:2004 table 3.1. [1]

Characteristics	**Units and values**	
Characteristic compressive cylinder strength of concrete at 28 days	f_{ck}	45 MPa
Design value of concrete compressive strength	f_{cd}	25.5 MPa
Characteristic axial tensile strength	$f_{ctk,0.05}$	2.70 MPa
Design value of axial tensile strength	f_{ctd}	1.53 MPa
Partial factor for concrete	γ_c	1.5
Young's modulus of concrete	E_c	36000 MPa

Table 1: Material characteristics concrete

The chosen prestressed reinforcement in the hollow core elements is of the type Y1860S7. MAKLADA PC STRAND TECHNICAL DATA [2] specifies requirements for high tensile strength steel products such as the chosen prestressed reinforcement. The most common prestressed reinforcement used in element production is Ø12.9 mm strands with a tensile strength of 1860 MPa. Ø12.9 consists of 7 wires tied together with a total nominal area of 100 mm^2. The characteristic 0,1% proof-stress of the prestressing steel, $f_{p0,1k}$ is 1640 MPa. Prestress information can be seen in Appendix B. The choice of which type of element and element height used depends on the project type. Figure 1, obtained from Betongelementboken bind A page 104 [3], show some of the most used elements that are produced:

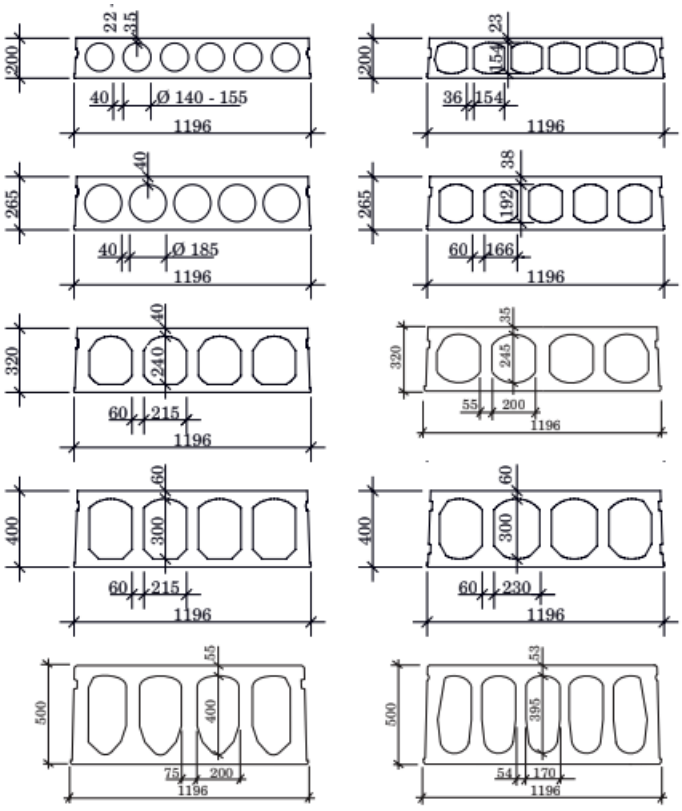

Figure 1: Hollow core cross-sections used in Norway.

2.2 General behavior of hollow core slabs

HCS is a prefabricated element that can resist both vertical and horizontal loads well and still maintain the necessary load distribution [3]. Displacements in the hollow core slab are mainly caused by dead load, live loads, and permanent loading. Due to this, the slab's geometry and cross-section is an important factor affecting the deflection caused by the loads. The requirements for the maximum deflection allowed for these elements are L/250 in the serviceability limit state according to EC2 7.4.1(4) p. 126 [1], but this requirement can be modified based on the project.

The diagram from Betongelementboken Bind A p. 105 figure A 7.2 [3], shown in figure 2, defines the load carrying capacity for HCS and shows the load that can be applied in the serviceability limit state in addition to the dead load. This load is based on several factors such as fire requirements, reliability, and load combination. The given load capacity is the upper limit when the maximum amount of reinforcement is allowed in the slab. So the load carrying capacity $\geq 0,90g + p$, where g is the dead load and p is the live load. The blue lines in figure 2 indicate that shear capacity will be the deciding factor limiting the allowed loading on the slab.

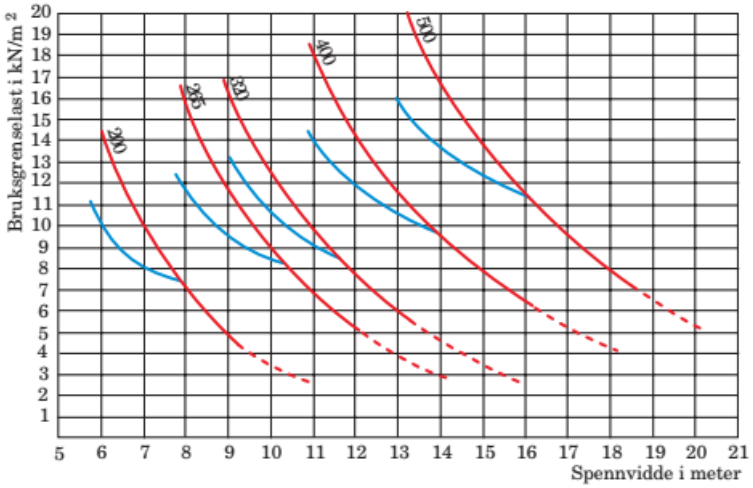

Figure 2: Load carrying capacity for hollow core slabs based on length and loading in the serviceability limit state.

The hollow core system will also experience some long-term deformations that limit the load carrying capacity. These deformations can result in upwards or downwards deflection depending on the prestress force and applied permanent loading. The immediate deflection when applying loads and prestress is the elastic deformation. Creep and relaxation are calculated based on the lifespan of the element and the applied load. The total deflection on the element is the sum of elastic deformation, creep, and relaxation. This is shown in figure 3 below, obtained from Betongelementboken bind A 4.2.1[3].

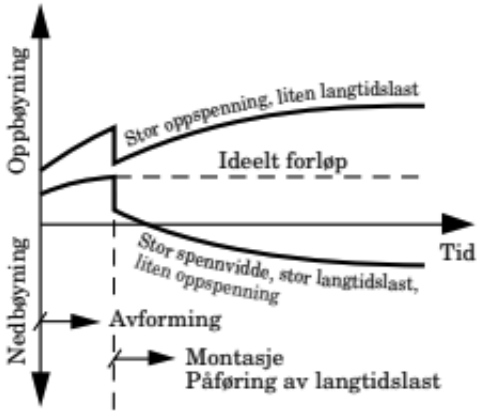

Figure 3: Deformation process in hollow core elements.

2.3 Load distribution between hollow core slabs

In order to discuss moments appearing in the HCS in the different directions, the terms transverse and longitudinal moments will be used in this thesis. Transverse bending moments are bending moments around the transverse axis, while the longitudinal bending moments are bending moments

around the longitudinal axis, also referred to as torsional moments.

Hollow core units are installed and tied together by cast concrete to make a close to monolithic system that allows load transfer between the slabs. The individual slab's load interaction allows the applied load to be distributed and shared across the entire system. This distribution is published and used by Betongelementforeningen in Norway. It is defined that line loads and concentrated loads can be distributed across the element's transverse direction. This distribution causes bending moments and vertical shear forces in the longitudinal joints between slabs. The cast joints are usually unreinforced, and therefore assumed cracked. With this assumption, the cracked joints can be considered linear hinges ([4], and [5]), and longitudinal moments will not be transferred between the slabs. The shear forces, however, are transferred in the joints. This hinge assumption has firm hold in the background theory from FIP articles and NS-EN 1168 [6], commented in the next section. In the FIB recommendations on precast prestressed hollow core slabs, Thomas Telford [5] states that shear forces will be transmitted across the cracks due to the presence of lateral compressive stresses originating from torsion of the elements and the sideways expansion due to the Poisson's effect. With no transverse reinforcement, the joints between the elements need to resist the resulting shear forces. This is explained more in detail in the following paragraphs.

Annex C in NS-EN 1168 [6] addresses the transverse load distribution on prestressed hollow core slabs. Two methods are presented in chapter C.1, the first method is load distribution based on theory of elasticity, and the other method is no load distribution. According to the first theory, the hollow core elements should be regarded as isotropic or anisotropic slabs with longitudinal joints considered as hinges. A requirement is to limit lateral displacements based on the requirement in C.3. Balconies apply concentrated forces on the edge of the outermost slab in the system. The distribution of this load depends on the load distribution factor α, which defines how much of the applied load distributed to each slab in the system. Figure C.3 in NS-EN 1168, Annex C [6], shown in figure 4 show α based on slab length and are calculated using theory of elasticity. The load distribution factor, α, for moment or deflection can be calculated when the moment or deflection profile for the system is obtained. These factors show the % distribution and can be calculated using the average displacement or moment for the i-th unit. The article: "Load distribution factors for hollow core slabs with in-situ reinforced concrete joints" by Kim S, Elliot [7] provides two equations to calculate these distribution factors. It is important to note that the flexural stiffness of the slab units (EI) in the transverse direction is assumed constant.

$$F_{mi} = \frac{M_i}{\sum_{i=1}^{5} M_i} \times 100 \tag{1}$$

$$F_{di} = \frac{\delta_i}{\sum_{i=1}^{5} \delta_i} \times 100 \tag{2}$$

For a concrete floor without cover, the load distribution factor needs to be increased by 25% for the load carrying element and reduced accordingly for the other elements. The diagram in figure 4 presents load distribution factors for concentrated loads. The diagram is still in use today for the calculation of load distribution on the precast system.

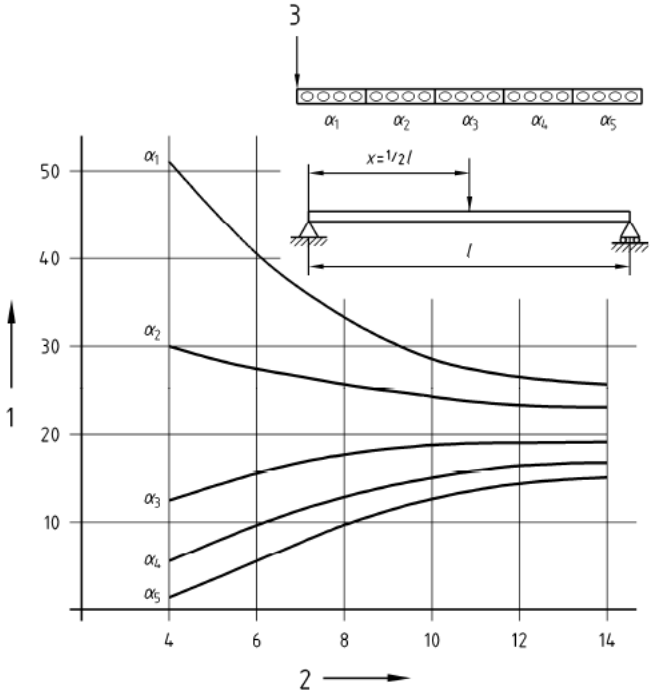

Figure 4: Load distribution factors for concentrated loads on the edge of a HCS system.

The placement of the load is important for the system response. Loads applied with eccentricity inflict moments and torsion. Deflection due to edge loads on the first slab causes the slab edges to deflect downward. This deflection is somewhat minimized by the concrete in the joints, and forces the adjacent slabs to deflect accordingly. The loaded slab's deflection is reduced due to the adjacent slab's stiffness. Torsional stiffness of the individual slabs also contributes to reducing the overall deflection of the system.

The second method assumes no load distribution in the system, leading to no shear force in the transverse joints, and the loaded element should be designed to handle the entire load distribution. In the ultimate limit state, the moments due to torsion and the load distribution in the transverse direction can be ignored. The effective width of the load should be determined according to C.2 in Annex C in NS-EN 1168 [6]. It is important to note that if the conditions in C.3 are not met, the effect of the load distribution should be ignored, and the elements are designed with the no load distribution method.

The FIP publication "Precast prestressed hollow core floors" from 1988 [5] explains the background for the presented transverse load distribution. Concentrated loads can be distributed in the system with background in isotropic slab theory. The joints should behave as hinges and have deflection

compatibility in the transverse and longitudinal direction, meaning that in connected points, the deflection must be similar. An analytical solution is presented in chapter 2.5.2 in the FIP report, assuming a cracked joint under the load, and presuming that the crack transfer the shear forces due to the already mentioned lateral compressive stresses caused by torsion. Graphs for load distribution similar to those in NS-EN 1168 can also be found in this chapter based on analytical calculations and empirical data, though the analytical calculations are not listed.

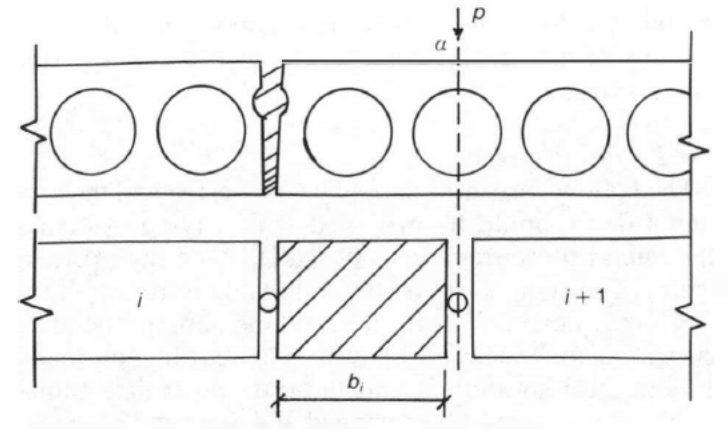

Figure 5: FIP assumption of a cracked hinge under the load in the ultimate limit state.

The assumption of a cracked joint below the load is also described in detail in the FIP publication "Transverse distribution of linear loading on prestressed hollow core floors" from 1984 [4]. Other general assumptions for this approach are that concentrated loading is presented as uniformly spread linear loading, longitudinal joints are acting as hinges, and the end bearing is supported with free supports. Figure 5 assumes full rectangular cross-section between the two hinges. The shear forces in the hinges are dependent on the torsional and transversal flexural stiffness of the elements.

The maximum load distribution capacity is in the ultimate limit state, and is reached when the first crack occurs in the hollow core slab. The load distribution is calculated by use of the mentioned analytical method in the ultimate limit state.

2.4 Shear

Shear failure in HCS can be categorized into three failure modes according to NS-EN 1168, 4.3.3.2.2.1 [6]. It can occur in both uncracked and cracked regions due to mainly bending. Anchorage failure can also occur if the crack arises within the anchorage length.

Loads near the joints yield shear forces in the neighboring slabs and the joints between the slabs. The shape of the shear forces in the joints can be seen in figure C.4 in NS-EN 1168. In this case, the shear capacity of the joints needs to be controlled. This control is done with the use of point

4.3.3.2.3 in NS-EN 1168 and figure C3.8 in Betongelementboken bind C [6][8]. The shear capacity for resisting linear load is the smallest value of the flange resistance v'_{Rdj} and the joint resistance v''_{Rdj}:

$$v'_{Rdj} = 0.25 f_{ctd} \sum h_f \tag{3}$$

$$v''_{Rdj} = 0.15(f_{ctdj} h_j + f_{ctdt} h_t) \tag{4}$$

The shear capacity resisting concentrated load is:

$$V_{Rdj} = v_{Rdj}(a + h_j + h_t + 2a_s) \tag{5}$$

Where v_{Rdj} is the smallest value of v'_{Rdj} and v''_{Rdj}. Figure 6 shows the values for determining the shear capacities.

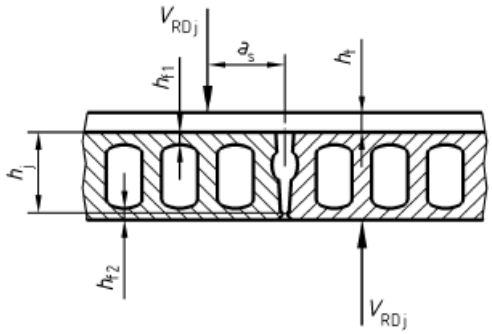

Figure 6: Dimensions in the HCS for calculating shear capacity.

HCS without concrete cover can also be subjected to punching shear. The concrete's ability to resist this point load failure is called punching shear resistance, V_{Rd}.

$$V_{Rd} = b_{eff} \cdot h \cdot f_{ctd}(1 + 0.3 \cdot \alpha \cdot \frac{\sigma_{cp}}{f_{ctd}}) \tag{6}$$

where $\alpha = \frac{l_x}{l_{bpd}} \leq 1$ according to 6.2.2(2) in Eurocode 2 [1], σ_{cp} is the concrete compressive strength at centrodial axis due to prestress, and b_{eff} is calculated based on failure due to concentrated loads from figure C3.9 in betongelementboken bind C 3.1.2.5 [8]. The figure is given below.

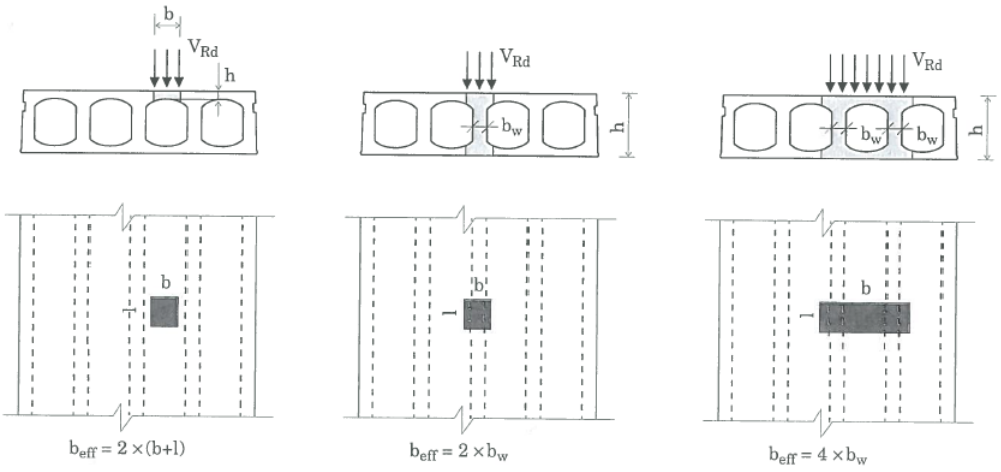

Figure 7: Calculation of b_{eff} for calculating punching shear.

According to NS-EN 1168, 4.3.3.2.4 [6], for concentrated loads where more than 50% is acting on the outermost web of a free edge of a slab, the resistance is divided by 2 if there is no transverse reinforcement present.

The HCS's ability to resist shear failure is directly dependent on the concretes tensile strength, f_{ctd}. With no transverse reinforcement, the concrete needs to resist this type of failure itself. Because of the low tensile resistance of concrete without reinforcement, this is an important factor to consider when designing HCS.

Another important factor in shear design of HCS is the capacity for resisting concentrated loads, F_k. According to 4.3.3.2.5 in NS-EN 1168, concentrated loads cause bending moments in the hollow core system. The tensile stresses due to bending moments need to be limited because of the lack of transverse reinforcement. Point loads affecting the hollow core slab system anywhere on the floor area is defined by F_k. Design assumptions include no load distribution, and loads affecting an element must be resisted by that element. This capacity is limited by the tensile stress $f_{ctk0,05}$ in the serviceability limit state, and W_l, the minimum section modulus in the transverse direction.

$$F_k = 3W_l f_{ctk0,05} \tag{7}$$

There is an exception when the hollow core elements are designed with elastic theory. Elastic theory distributes the load to adjacent elements, and limits the value of the tensile stress to f_{ctd} in the ultimate limit state. The capacity for resisting concentrated loads in ULS is:

$$F_d = 3W_l f_{ctd} \tag{8}$$

2.4.1 Web shear strength

Shear cracks in the webs are a failure mode that occurs due to the lack of shear reinforcement. It is assumed that the shear stresses caused by vertical shear are distributed over all the webs. When the max principal stress, σ_I, in the webs is larger than the uniaxial tensile strength of the concrete, f_{ct} a shear crack is formed. The crack forms at a 45° from the support to the intersection at mid plane according to research done by Mercx and Walraven [2]. Here, the shear stress, τ_v imposed by the load is:

$$\tau_v = \frac{V \cdot S}{\sum b_w I} \tag{9}$$

The stress state in the web is simplified to be two-dimensional. This means that an approximation for the principal stress consists of the horizontal normal stress and shear stress. The principal stress in the web due to compression is small, and will not influence the tensile strength of the web in the transverse direction (crushing). The maximum principal stress and failure criterion is therefore:

$$\sigma_I = \frac{\sigma}{2} + \sqrt{\left(\frac{\sigma}{2}\right)^2 + \tau^2} = f_{ct} \tag{10}$$

Using this failure criterion, 4.3.3.2.2.2 in NS-EN 1168 defines the shear capacity for web shear tension failure as:

$$V_{Rdc} = \frac{I \sum b_w}{S} \sqrt{(f_{ct}^2 + \alpha \sigma_{cp} f_{ct})} \tag{11}$$

2.5 Torsion

Torsion is caused by eccentric vertical shear forces causing a rotation of the slab. This torsional loading causes shear stresses in the flanges and outermost webs together with normal stresses due to bending moment and prestressing. Cracks can start either in the webs or in the flanges depending on the thickness of the cross section and the combination of these stresses. Shear stress caused by torsion is given by the torsional moment, T, and transformation of the HC slab to a tubular cross-section given by W_t.

$$\tau_T = \frac{T}{W_t} \tag{12}$$

$$W_t = 2t \left[h - \frac{(t_{top} + t_{bottom})}{2} \right] (b - b_{w,out}) \tag{13}$$

The formulas and transformations is given in a research by K. Lundgren [3]. The thickness, t, can not be larger than A/u. u is the circumference of the transformed cross-section, and A is the cross-sectional area.

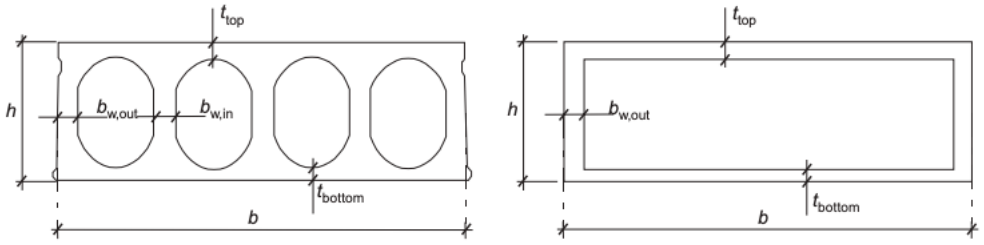

Figure 8: Transformation of hollow core unit cross-section into a tubular cross-section, Magazine of Concrete Research, 2005, 57, No. 9.

Also in torsion, the tensile strength of concrete limits the stresses on the cross-section in the ultimate limit state. The torsional capacity of the top flange and web is given by, $T_{R,top}$ and $T_{R,web}$, and assumes that cracking of the top flange or web results in failure.

$$T_{R,top} = W_{t,top}\sqrt{(f_{ct}^2 + \sigma_c f_{ct})} \tag{14}$$

$$T_{R,web} = W_{t,web}\sqrt{(f_{ct}^2 + \alpha\sigma_{cp} f_{ct})} \tag{15}$$

2.6 Shear and torsion interaction

Shear capacity of a hollow core element when subjected to torsion:

$$V_{Rdn} = V_{Rd,c} - V_{Etd} \tag{16}$$

where

$$V_{Etd} = \frac{T_{Ed}}{2b_w} * \frac{\sum b_w}{(b - b_w)} \tag{17}$$

$V_{Rd,c}$ is the design value of shear resistance according to 6.6.2 of NS-EN 1992-1-1:2004 [1]. When torsional moments affect the system, they reduce the overall shear capacity of the hollow core elements. This is important to note when applying eccentric loads that introduce shear forces of different magnitude that result in torsional moments in the system. When considering shear and torsion affecting a non-solid cross-section like a hollow core slab, the web closest to the edge is subjected to shear stresses from shear forces and torsion, namely, τ_V and τ_T.

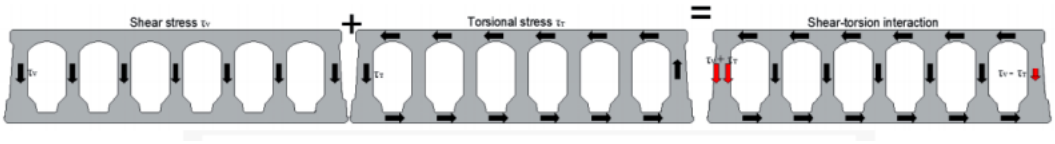

Figure 9: Distribution of the tangent stresses, W. Derkowski, Torsion of precast hollow core slabs, Cracow University of Technology, 2015 [9].

2.7 Non-rigid supports

Hollow core slabs supported on rigid beams with uniform and symmetrically distributed loading make a 2-dimensional stress distribution assumption valid. Parallel supports and no angle means that no torsional stresses act on the construction [**?**]. When the supports have a more moderate stiffness, the support beam will deform and cause a composite effect between the beam and slab. This composite action causes transverse stresses in the slab that need to be accounted for in the design process.

The transverse stresses cause a shear flow in the webs in addition to the shear flow that acts when the slabs are on rigid supports. This shear flow is dependent on the imposed load. [FIB, s. 90] This load acts after the cast concrete in the joints have hardened. Cracks can occur in the flange, which is in the tensile zone of the slab and is more at risk where there is reinforcement. These cracks can directly affect the bond between reinforcement and concrete and reduce the capacity of the slab due to reduced prestress. The design criterion is the same for these types of failures as for the web shear failure. Because of the lack of reinforcement, the failure occurs when the concrete's characteristic tensile capacity is smaller than the maximum principal tensile stress. Nevertheless, the additional shear stress depending on the beam and support type still has to be considered: [FIB, s. 92]

$$\sigma_I = \frac{\sigma}{2} + \sqrt{\left(\frac{\sigma}{2}\right)^2 + \tau_1^2 + \tau_2^2} = f_{ct} \tag{18}$$

The composite action causes transverse horizontal shear stresses along the beam axis in the webs and the compressive and tensile behaviors in the flanges. The vertical shear stresses combined with the horizontal reduces the slab's shear capacity on rigid supports compared to the opposite.

2.8 Edge anchorage

When anchoring steel strands or plates at the edge of the hollow core slab, the tensile stresses have to be smaller than the tensile strength of the concrete. Here, the concrete is thin, and failure can result in severe damage to the structure because the failure is brittle and without warning due to the lack of transverse reinforcement. Tensile failure over the voids is dependent on the design tensile strength. In reality, the flanges over and under the voids cannot fail at the same time. Therefore the design only accounts for one of them failing. Betongelementboken bind C, 12.3.1 [8], defines the upper boundary for design loading for edge anchorage, $s_{d\emptyset}$:

$$s_{d\emptyset} = 0.5 f_{ctd} t \tag{19}$$

The upper boundary is dependent on the thickness of the concrete over the voids, t. This thickness is different based on both the hollow core element manufacturer and the type of element i.e., 200mm HCS, 265mm HCS, or 320mm HCS. The tensile forces applied will almost always be concentrated loads. The biggest force that can be anchored in the hollow core element is $S_{Rd,c} = s_{d\emptyset} \cdot s$, where

s is the length between the concentrated loads. The hollow core element can fail in the different void channels. The part in tension will be torn out of the element. The capacity decides how far in the element the concentrated load needs to be anchored. The previously mentioned 12.3.1 in bind C has a table determining anchor length and center distance between the concentrated loads. Figure 10 show the failure mechanism when the hollow core element is loaded with a concentrated horizontal load.

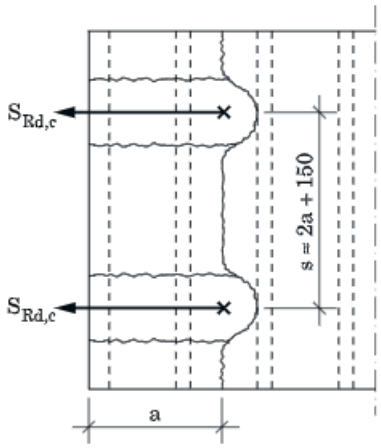

Figure 10: Failure mechanism for HCS applied horizontal concentrated loads on the edge.

2.9 Principal stresses

In this thesis, the hollow core slabs are analyzed to figure out the largest principal tensile stresses appearing on the backside of the applied concentrated load. The principal stresses are peak values for the normal stress working on a body in a single point and will work with an angle of 90 degrees on each other. In any situation with compound stresses acting on a body, a particular configuration will be given with a rotation that will give only normal stresses on the body. This configuration will be the configuration of principal stresses, and there will be no shear stresses present. To figure out whether the principal tensile stresses will cause cracks or not, the stresses will simply be compared with the value for the tensile strength of concrete.

In cases where 3D models are analyzed, principal stresses will be appearing in three directions. The acting principal stresses will, as always, be 90 degrees on each other. Principal stresses on the edge of a body will be a special case for principal stresses in a 3D model. Here, the principal stresses appear in the directions tangential to the surface of the point where the principal stresses are calculated. There will be no stresses acting perpendicular to the surface. Below, a figure shows how the principal stresses may act on a point in a body in 2D.

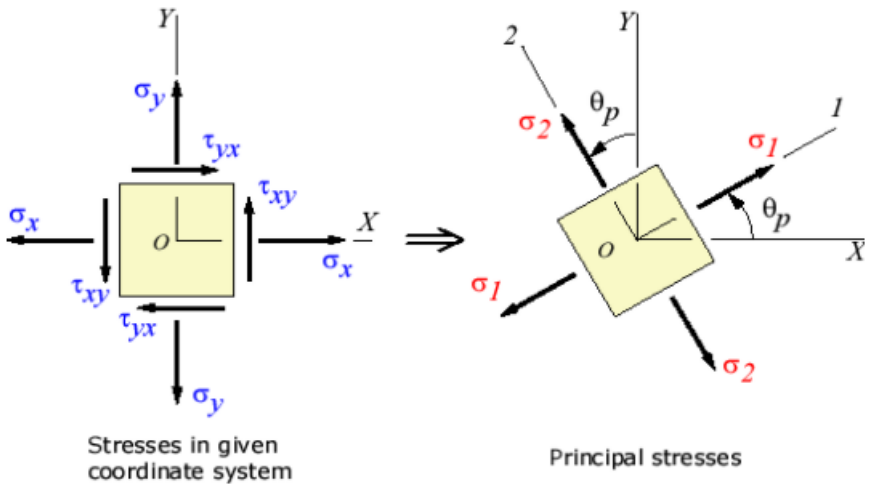

Figure 11: Transformation of stresses from a given coordinate system to principal stresses.

2.10 Previous research

A. Aswad and F. J. Jacques published a PCI journal regarding the behavior of HCS subjected to edge loading [13]. Tests of 25 hollow core slab specimens subjected to different edge loadings and their resulting failure modes. Web shear failure, shear-torsion, punching shear, and end shear were among the resulting failure modes. These tests are taken into consideration when modeling our problem. Matti Pajari [14] has also conducted comprehensive testing on hollow core slabs to check the failure modes. His publications proved helpful when getting insight on hollow core slabs' behavior and failure modes when subjected to load. H. Broo published in 2005 an article on finite element analyses of hollow core slabs subjected to shear and torsion, where tests of hollow core slabs were compared to a finite element model made in Abaqus/CAE [10]. This publication proved helpful in making the right choices regarding our finite element model. The FIP publication precast prestressed hollow core floors, Thomas Telford from 1988 [5], was used to describe and model the behavior of the load distribution and hollow core slab system. Furthermore, the FIP publication transversal distribution of linear loadings in prestressed hollow core floors, A. Van Acker from 1984 [4], was used to investigate further and describe the load distribution.

Jong-Young Song and Kim S, Elliott published the article Load Distribution Factors for Hollow Core Slabs with In-situ Reinforced Concrete Joints which showed calculated load distribution factors for a loaded hollow core slab floor system, comparing them to the load distribution factors calculated in NS-EN 1168 [7].

3 Methodology

The methodology in this task was first to do a literature study to identify the relevant research related to the problem. Existing studies done on hollow core slabs and concrete itself were important before analyzing the problem of concentrated load applied to the edge of a hollow core slab. To analyze this problem, information about the stress distribution in a system of hollow core slabs was needed. The hollow core standard NS-EN 1168 [6], and research done by the hollow core group in FIP [4], [5] presented valuable data related to the current problem.

The previous research was critically analyzed to find a basis for design. To understand how the HCS behave, it was important to consider the effect of load distribution in the mentioned studies and research. A load distribution model was then established and analyzed. The results were used to make a correct representation of a system of HCS, although only a single hollow core slab was modeled and analyzed.

A linear elastic analysis was performed for the main task to investigate the capacity of the slab in the transverse direction, where the hollow core slabs are not reinforced. This type of analysis seems suitable as the concrete performs as a linear material with a constant Young's modulus until the material cracks. Since the concrete is not reinforced in the transverse direction, the failure of the material will also happen when the concrete cracks.

3.1 Load distribution model

The load distribution model was created to replicate or understand how the concentrated edge load distributes across the hollow core slab system. The system consists of five 1200mm slabs connected by four 30mm concrete joints and can be seen in figure 12.

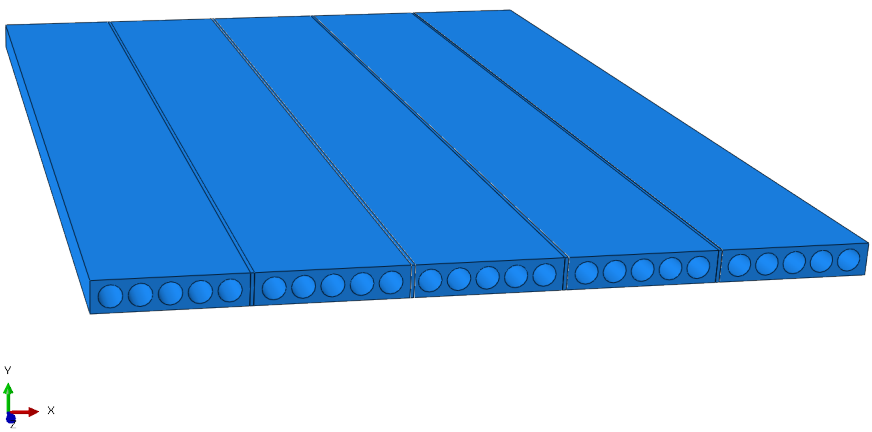

Figure 12: Hollow core floor system consisting of five slabs and cast concrete joints.

The first method mentioned in C.1 from annex C in NS-EN 1168 was the basis for the model and the diagrams. The properties of the hollow core slab were assumed isotropic, with the same stiffness in both directions as mentioned in the FIP report from 1988[5]. Elastic analysis was performed as it is interesting to see how the loads distribute in the slab system before any cracks occur. This is because the concrete will behave almost perfectly linear elastic until a crack occurs. Since the hollow core slab is unreinforced in the transverse direction, a crack in the longitudinal direction over the voids is critical, and the design conditions will therefore assume the concrete in the HCS to be free of cracks. The Young's modulus is therefore assumed constant in all the analyses. The grouted joints between the hollow core slabs are assumed to be of quality C25 concrete, unlike the concrete in the hollow core slab, C45. The cast joint is assumed to be cracked in the longitudinal direction, acting as a hinge, as stated in the FIP theory and NS-EN 1168 to fulfill the load distribution assumption. The concrete in the hollow core slab is not assumed to be cracked in the area below the load, as recommendations from FIP. This is because the load is situated on the edge of the slab.

3.2 Local failure model

The main focus of this thesis is to examine the tensile stresses developing on the top side of the HCS due to the concentrated load on the edge of the slab. The problem is analyzed and described by many different cases and parameters to see their impact on tensile stresses on the top of the hollow core slab. Analyses are done on three different HCS, with thicknesses of 200mm, 265mm, and 320mm. Dimensions for the different hollow core slab types used in the analysis can be seen in figure 13, 14, and 15. The slabs have their cross-sections modified with completely straight edges to ease the modeling process.

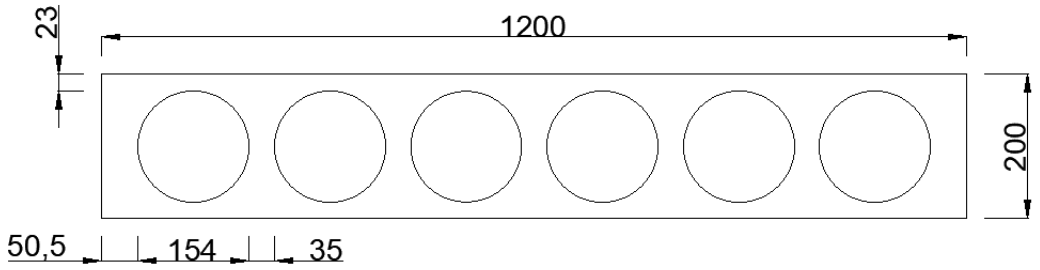

Figure 13: Cross-section used for modelling the 200mm HCS.

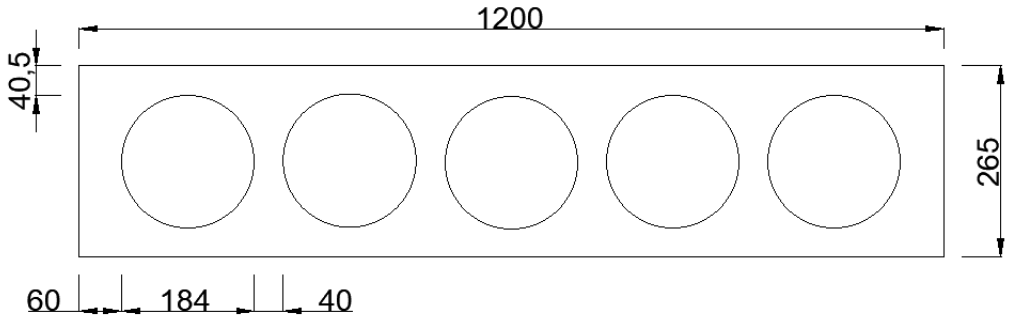

Figure 14: Cross-section used for modelling the 265mm HCS.

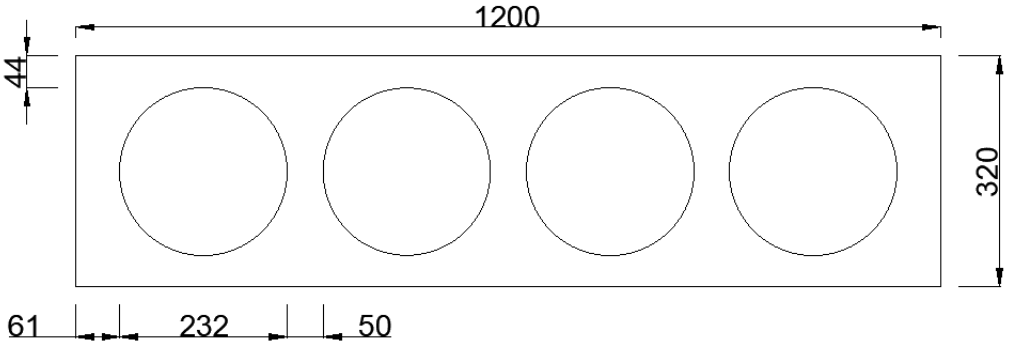

Figure 15: Cross-section used for modelling the 320mm HCS.

The different hollow core slabs have the two outermost voids filled with concrete, over a length of 250mm, to increase the capacity and connect the balcony. Although the amount and size of the voids are different for the different HCS, there are still just the two outermost hollow cores that are filled with concrete.

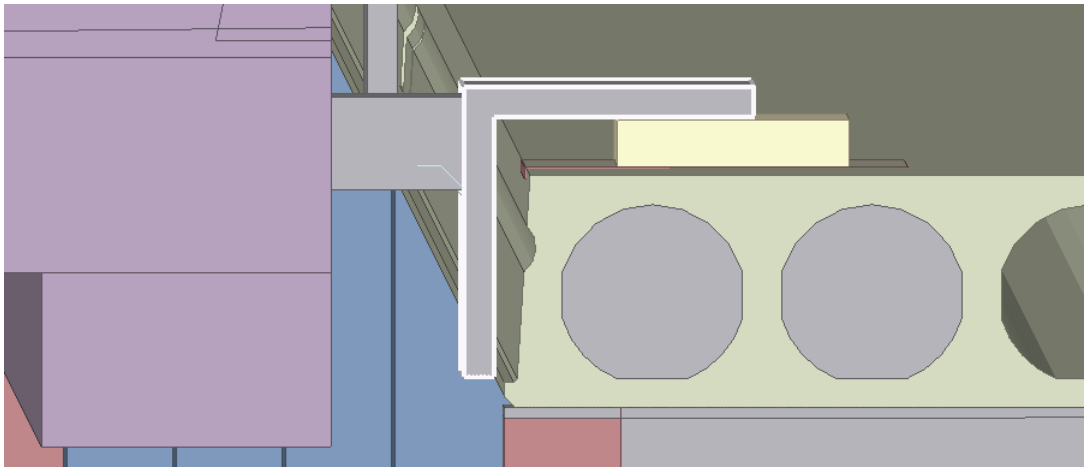

Figure 16: Example of how the outer voids are filled with cast concrete to connect the balcony.

Two different balcony sizes are used to decide the concentrated load used in the analysis of this thesis. Both balconies are made of concrete, and the size of them is 4.2x2.2mx0.22m for the small one and 7.2x2.5mx0.22m for the large one. The concentrated loading is applied in the center of the span and 1000mm from the slab's support to see the different effect the location of the load has on the tensile stresses. The dimensions of the two different balconies applied to the slab system can be seen in figure 17 and 18.

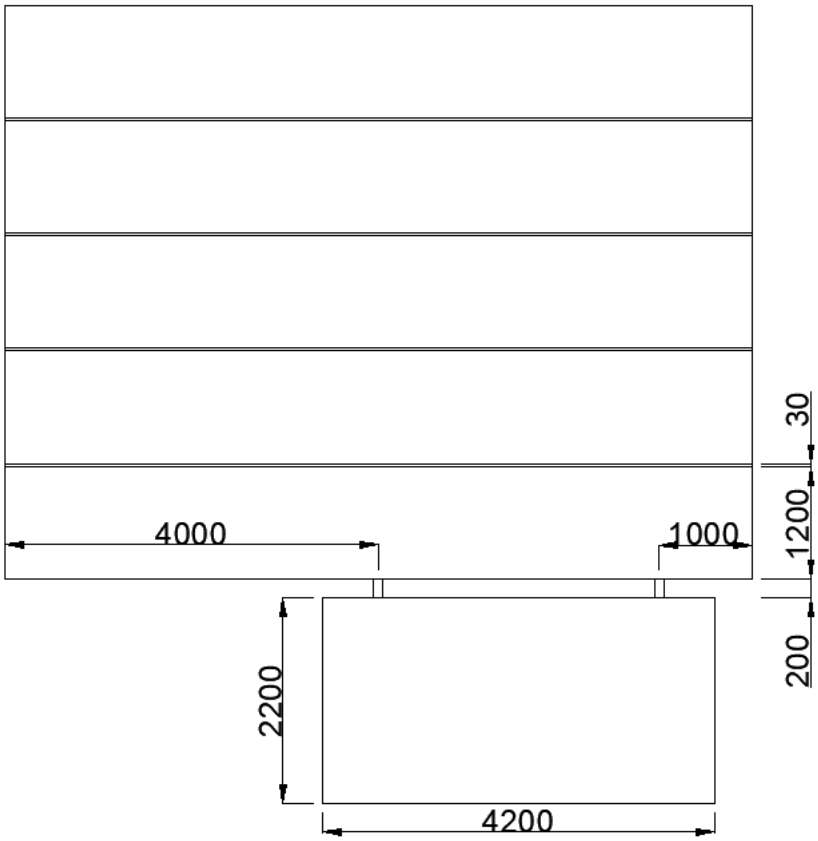

Figure 17: Dimensions of the HCS system applied a small balcony.

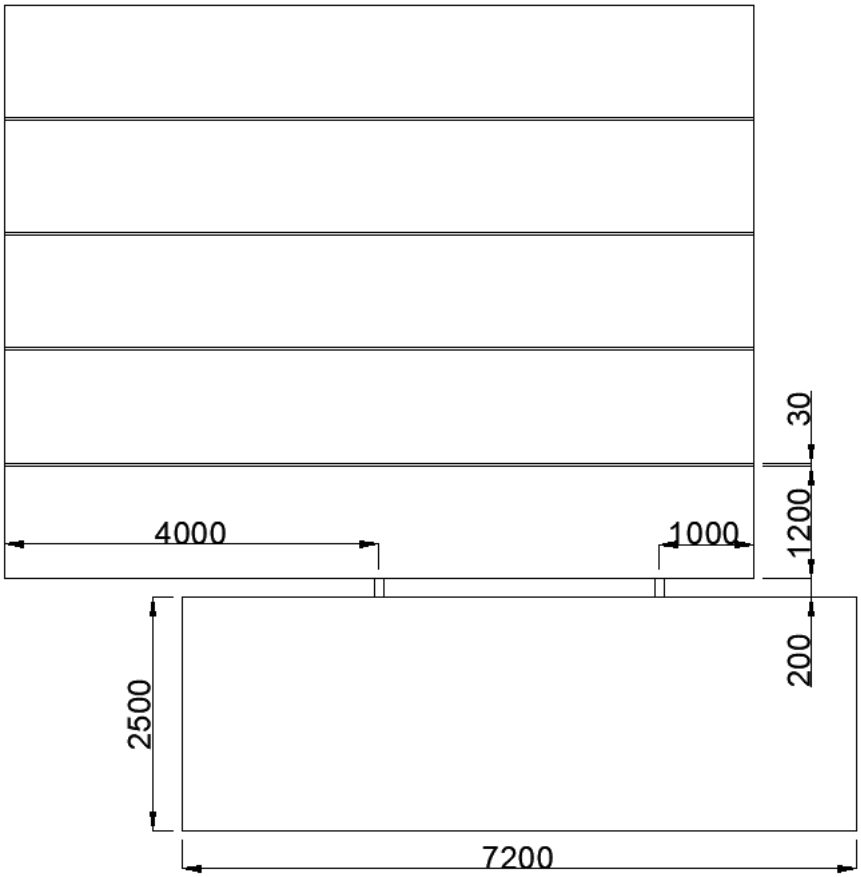

Figure 18: Dimensions of the HCS system applied a large balcony.

3.2.1 Parameter variation

A steel plate is integrated into the system and placed 25mm below the loaded area. The reason for this is to distribute the concentrated load better into the hollow core slab in order to avoid large concentrated stresses right behind the applied load. Analyses are done with the placement of the steel plate at different depths to estimate the effect on the principal tensile stresses behind the applied load. Every slab type is analyzed with the maximum amount of reinforcement bars in the bottom of the hollow core slab according to what is standard in the industry in Norway.

SPENNTAUMØNSTER HD200 OG HD220

Spenntau OK	I	II	III	IV	VI
0					
1			X		
2		X		X	
3	X		X		X
4	X	X	X		X
5	X	X	X	X	X

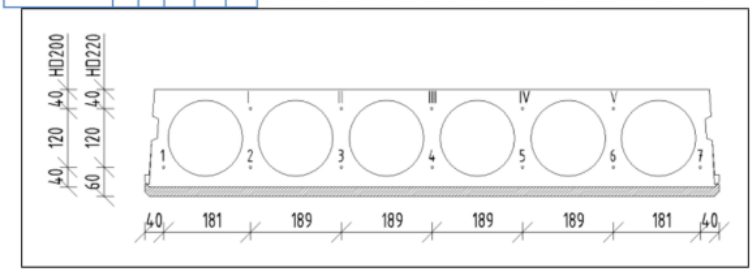

Spenntau UK	1	2	3	4	5	6	7
5	X	X		X		X	X
6	X	X	X		X	X	X
7	X	X	X	X	X	X	X

Figure 19: Amount and placement of the reinforcement bars in the 200mm HCS.

SPENNTAUMØNSTER HD265 OG HD285

Spenntau OK	I	II	III	IV
0				
1			X	
2	X			X
3	X		X	X
4	X	X	X	X

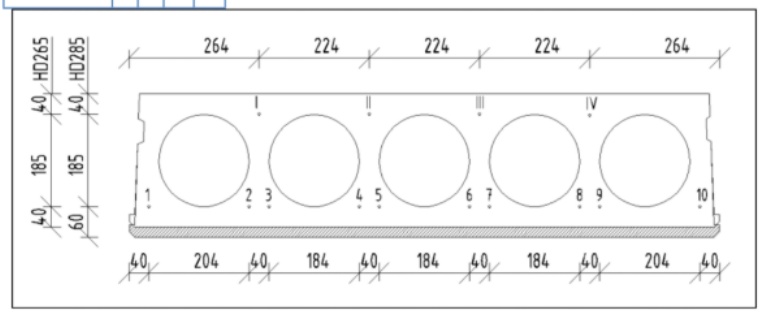

Spenntau UK	1	2	3	4	5	6	7	8	9	10
3	X				X					X
4	X			X			X			X
5	X	X		X			X			X
6	X	X		X			X		X	X
7	X	X		X	X		X		X	X
8	X	X		X	X	X	X		X	X
9	X	X	X	X	X	X	X		X	X
10	X	X	X	X	X	X	X	X	X	X

Figure 20: Amount and placement of the reinforcement bars in the 265mm HCS.

SPENNTAUMØNSTER HD320 OG HD340

Spenntau OK	I	II	III
0			
1		X	
2	X		X
3	X	X	X

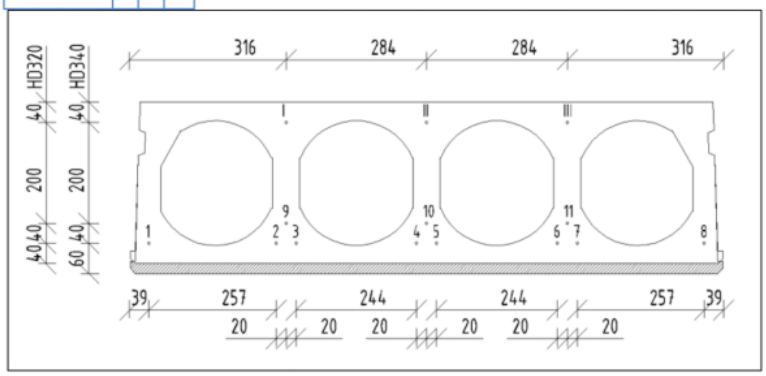

Spenntau UK	1	2	3	4	5	6	7	8	9	10	11	a_m
5	X		X		X	X		X				40/60
6	X	X		X	X		X	X				40/60
7	X	X	X	X	X		X	X				40/60
8	X	X	X	X	X	X	X	X				40/60
9	X	X	X	X	X	X	X	X		X		45/65
10	X	X	X	X	X	X	X	X	X		X	48/68
11	X	X	X	X	X	X	X	X	X	X	X	48/68

Figure 21: Amount and placement of the reinforcement bars in the 320mm HCS.

The maximum amount of reinforcement bars seen from figure 19, 20, and 21 is 7 reinforcement bars for the 200mm HCS, 10 bars for the 265mm HCS and 11 bars for the 320mm HCS. No reinforcement bars are implemented in the top of the slab. In order to analyze the effect that the varying amount of reinforcement bars has on the tensile stresses behind the concentrated load, the 265mm HCS is analyzed with 8, 7, and 4 bars in the bottom as well. In addition, the numerical errors related to the mesh size need to be quantified. This will be done by analyzing the same HCS with different mesh sizes and look at the stresses to see how they are affected.

3.2.2 Loads applied to the model

The analysis is done in ultimate limit state, and according to NS-EN 1990 [15] some factors for loading need to be used to analyze the correct loading on the hollow core slab. According to the standard, design values for loads should be decided in persistent and transient situations. In this case, the self-weight of the balcony itself can be assumed persistent, and the live load on the balcony can be assumed transient. According to the standard, the load factor for permanent self-weight should be 1.35 because it is not favorable. The same account for the live load, being non-favorable, but the load factor is 1.50 because it is a dominating variable load.

Table A1.2(A) - Design values of actions (EQU) (Set A)

Persistent and transient design situations	Permanent actions		Leading variable action (*)	Accompanying variable actions	
	Unfavourable	Favourable		Main (if any)	Others
(Eq. 6.10)	$\gamma_{G,j,sup} G_{k,j,sup}$	$\gamma_{G,j,inf} G_{k,j,inf}$	$\gamma_{Q,1}\ Q_{k,1}$		$\gamma_{Q,i}\ \psi_{0,i} Q_{k,i}$

(*) Variable actions are those considered in Table A1.1

NOTE 1 The γ values may be set by the National annex. The recommended set of values for γ are :

$\gamma_{G,j,sup} = 1{,}10$

$\gamma_{G,j,inf} = 0{,}90$

$\gamma_{Q,1} = 1{,}50$ where unfavourable (0 where favourable)

$\gamma_{Q,i} = 1{,}50$ where unfavourable (0 where favourable)

NOTE 2 In cases where the verification of static equilibrium also involves the resistance of structural members, as an alternative to two separate verifications based on Tables A1.2(A) and A1.2(B), a combined verification, based on Table A1.2(A), may be adopted, if allowed by the National annex, with the following set of recommended values. The recommended values may be altered by the National annex.

$\gamma_{G,j,sup} = 1{,}35$

$\gamma_{G,j,inf} = 1{,}15$

$\gamma_{Q,1} = 1{,}50$ where unfavourable (0 where favourable)

$\gamma_{Q,i} = 1{,}50$ where unfavourable (0 where favourable)

provided that applying $\gamma_{G,j,inf} = 1{,}00$ both to the favourable part and to the unfavourable part of permanent actions does not give a more unfavourable effect.

Figure 22: NS-EN 1990, Table A1.2(A).

Additionally, different variations of the eccentricity moment from the balcony are applied to the hollow core slab to see the impact the possible moment has on the tensile stresses.

3.2.2.1 Vertical forces from the balconies

The main load for the analysis in this project is the concentrated vertical force from the load of the balcony with the belonging live load on the balcony. Two different vertical loads are applied with the background of the two different balconies discussed earlier in the chapter. The balconies are in both cases supported by columns on the opposite side of the balcony connections in the hollow core slab. The balconies are assumed to be of solid concrete, and in addition to the self-weight of the concrete being equal to 24kN/m^3, the live load on the balcony is assumed to be 4kN/m^2. From the previous chapter, presenting the load factors, the total vertical load calculated from the smallest of the balconies will be 30.3kN, and the calculation of the largest load will be 59.1kN. The highest value is assumed to be in the limit area of what the connection can withstand.

3.2.2.2 Horizontal forces from the balconies

Various horizontal loads from the balcony on the hollow core slab need to be considered. In this thesis, wind loads and loads from the eccentricity of the columns supporting the balcony are calculated. The design value for the wind loads acting on the balcony depends on the location of the construction. The limits for the wind loads are therefore taken from the most and least windy cities in Norway. From the National annex of the NS-EN 1991 [16], a minimum wind value was found for Oslo with a maximum wind speed of 22m/s, while Bodø was the windiest city in Norway with a maximum wind speed of 30m/s. The maximum and minimum wind loads were therefore calculated with the basis of these wind speeds. According to Invisible Connections, the maximum inclination of the columns can be assumed to be 0.5%. Together with the wind loads acting on the balcony's railing, this makes up the total horizontal load acting on the hollow core slab from the balcony. The maximum loading for suction due to wind is $0.47kN/m^2$, and $1.3kN/m^2$ is found from EC1-1-4 based on the wind condition from Oslo and Bodø. Based on information from the industry, the railing is assumed to be 1200mm, and the loads are calculated using the two balconies mentioned above. As previously mentioned, the live load applied to the balcony is assumed $4.0kN/m^2$. This gives an inclination load of:

$$H_{0.5\%} = \left[\frac{t \cdot b \cdot d \cdot \rho_c}{2} \cdot 1.35 + \frac{liveload \cdot b \cdot d}{2} \cdot 1.5\right] \cdot 0.005 \tag{20}$$

$H_{0.5\%,smallbalcony} = 0.264$ kN
$H_{0.5\%,largebalcony} = 0.514$ kN

Horizontal load due to suction from wind, small balcony:
$H_{wind,min} = 0.47kN/m^2(1.2m + 0.25m) \cdot \frac{4.2m}{2} = 1.43kN.$
$H_{wind,max} = 1.3kN/m^2(1.2m + 0.25m) \cdot \frac{4.2m}{2} = 3.96kN.$

Horizontal load due to suction from wind, large balcony:
$H_{wind,min} = 0.47kN/m^2(1.2m + 0.25m) \cdot \frac{7.2m}{2} = 2.45kN.$
$H_{wind,max} = 1.3kN/m^2(1.2m + 0.25m) \cdot \frac{7.2m}{2} = 6.8kN.$

Total horizontal load:
$H_{small,min} = 1.7kN$
$H_{small,max} = 4.2kN$
$H_{large,min} = 3.0kN$
$H_{large,max} = 7.3kN$

Table C12.7 from Betongelementboken bind C, 12.3.1 show calculated values for the maximum horizontal load that can be anchored in the slabs. The calculated horizontal loads above are far from exceeding these capacities.

3.2.2.3 Loads from the prestressed reinforcement

In the serviceability limit state for prestressed precast hollow core slabs, it is assumed that the concrete remains uncracked. According to Eurocode 2 [1] the maximum allowed prestress applied to the reinforcement is $0.9f_{p0,1k}$. Overstressing is also allowed if the prestress force can be measured with a $\pm 5\%$ accuracy in the jack, then a stress of $0.95f_{p0,1k}$ is allowed.

The stresses applied to the concrete immediately after the prestress transfer should be limited to $0.85f_{p0,1k}$. This limitation is not applied for hollow core slabs, where it is normal to limit the stresses to $0.7f_{p0,1k}$ not to utilize the total capacity. Due to immediate losses like shrinkage, this stress is reduced to $0.63f_{p0,1k}$. This value is based on instructions from the industry and supervisors to take losses into account. A prestress force in each cable of 100kN is given from a hollow core manufacturer. Compared to the calculated value of P_0', the stresses applied to the reinforcement are reasonable to assume.

To obtain the prestress force, the strain in the reinforcement is calculated. It's stated that the stresses applied to the reinforcement in the HCS after losses is $0.63f_{p0,1k}$. The strain is then equal to:

$$\epsilon_{p0}' = \frac{0.63f_{p0,1k}}{E_p} = \frac{0.63 \cdot 1640MPa}{195000MPa} = 5.298 \cdot 10^{-3} \tag{21}$$

This strain is then used to calculate the prestress force in each strand:

$$P_0' = \epsilon_{p0}' \cdot E_p \cdot A_p = 5.298 \cdot 10^{-3} \cdot 195000MPa \cdot 100mm^2 = 103.320kN \tag{22}$$

The prestress can also be calculated and applied with thermal strains. The thermal expansion coefficient for steel is between 11 to $13{\cdot}10^{-6}K^{-1}$. In order to calculate the temperature difference applied to the reinforcement, the thermal strain is set equal to the strain caused by the prestress force. In this way, the prestress can also be modeled using thermal strains.

$$\epsilon_{\Delta T} = \alpha_T \cdot \Delta T = \epsilon_{p0}' \tag{23}$$

$$\Delta T = \frac{\epsilon_{p0}'}{\alpha_T} = \frac{5.298 \cdot 10^{-3}}{12 \cdot 10^{-6}K^{-1}} = 441.5K \tag{24}$$

3.2.2.4 Shear forces due to system behavior

Although the shear force is distributed continuously along the longitudinal joint as shown in figure 43, the difference compared to applying five traction forces of varying magnitude is assumed to be low. The traction forces applied are an averaged value distributed over multiple areas of the longitudinal edge of the single hollow core slab. Additionally, when the non-continuous distribution applied on the hollow core slab is conservative, it will not show tensile stresses close to the concentrated load which are lower than in reality. The non-continuous load distribution of the shear force is assumed conservative because behind the concentrated load, shear stresses in the joint

reach the maximum value. The shear stresses applied to the hollow core slab are lower behind the concentrated load because it results from an averaged shear force over a larger area. When the upward shear force applied to the longitudinal edge of the hollow core slab is lower, it causes lower compression forces in the transverse direction on the top side of the hollow core slab because of the torsional moment created. The same accounts for the hollow core slab loaded with two concentrated loads. In this case peaks for the friction forces in the joint appears almost right behind the concentrated load with a slight deviation due to the non-symmetry of the system. However, the stresses applied to the hollow core slab behind the concentrated load are still a result of an averaged value over a larger area and lower than the actual upward friction stresses. Therefore these loading conditions can be seen as conservative, as the compression forces created from the traction forces is lower than what it would have been with the distribution shown in figure 45. Calculated values of the uniform traction loads are given in Appendix D.

3.2.2.5 Moment due to connection detail

An important factor affecting the tensile forces in the top flange of the slab is the balcony to hollow core slab connection. The connection details are important when determining the load details applied to the local failure model. Two connection examples are shown in appendix D, the BWC 55 and BWC 55 light made by Invisible Connections. The two solutions are just examples of how it can be done, but other connection suppliers/manufacturers may deliver different details. The balcony will be loaded with live load, potential snow load, installations, and self-weight. Depending on the balcony size, this vertical loading affecting the connection can be very close to the vertical capacity of the connection. This vertical force will be transferred to the hollow core slab through this connection detail, as seen in figure 51.

Depending on the details of the connection, an eccentricity moment may be transferred from the balcony to the HCS. This moment depends on whether the connection is fixed to the balcony slab or the hollow core slab itself. If the connection is fixed to the hollow core slab, it means that an eccentricity moment needs to be accounted for. Because the connection may be partly fixed in both ends, analysis is done with the hollow core slab exposed to 0%, 20%, 50%, and 100% of the total eccentricity moment. With this assumption, the balcony slab will be exposed to a moment of respectively 100%, 80%, 50%, and 0% of the total eccentricity moment. The eccentricity distance used in the calculations is 200mm, and this is the distance assumed to appear between the hollow core slab and the balcony. The possible connection types analysed in this thesis between a balcony and HCS are:

- Pinned - Fixed (0-100)
- Fixed - Fixed (20-80)
- Fixed - Fixed (50-50)

- Fixed - Pinned (100-0)

With these connection types, this moment can either be distributed in the hollow core slab or in the balcony, or both. The moment magnitude is dependent on both the balcony size and connection length. Therefore it is vital to consider the effect of this moment when analyzing the results.

4 Finite element modeling

4.1 Software

In order to get accurate results, the model was made in the finite element analysis program Abaqus/CAE. This software is used for modelling and analysis of advanced mechanical parts, while being able to visualize the results. Finite element analysis is used because it is an excellent way to analyze complex geometries. Additionally, it can adapt to most requirements or prerequisites, it has a high degree of accuracy, and it yields results closely correlated to theory. It is also great because of its ability to visualize the problem and results.

Two types of analyses are performed in Abaqus/CAE. The first analysis is of how concentrated load is distributed in a system of HCS. The other analysis controls tensile stresses in the top flange of a single hollow core slab exposed to a concentrated edge load. The two analyses are modeled, explained, and pictured in the following chapters.

4.1.1 Modeling approach

Abaqus/CAE has no standard units, but are consistent with either SI units or US units depending on the users preference. Here, SI (mm) are used as the units. The following unit system was used in this context.

Quantity	**SI**	**SI(mm)**
Length	m	mm
Force	N	N
Mass	kg	$tonne(10^3 kg)$
Time	s	s
Stress	$Pa\ (N/m^2)$	$MPa\ (N/mm^2)$
Energy	J	$mJ\ (10^3\ J)$
Density	kg/m^3	$tonne/mm^3$

Table 2: SI units used in the Abaqus/CAE model.

Element types in Abaqus/CAE are defined by multiple aspects that characterize the behavior. These aspects are essential to understand when choosing the correct element type to model the behavior wanted and obtain accurate results from the analysis. Important aspects are:

- Element family
- Degrees of freedom

- Number of nodes
- Formulation
- Integration

The different element families can be seen in figure 23 from the Abaqus User Manual chapter 27.1.1-1 [17]. The families are used to describe the element type and behavior. Classification of the families is done by using the element name, where the first letter or letters are used to indicate which family the element belongs to. For example, S4R is a shell element, and C3D8R is a continuum element.

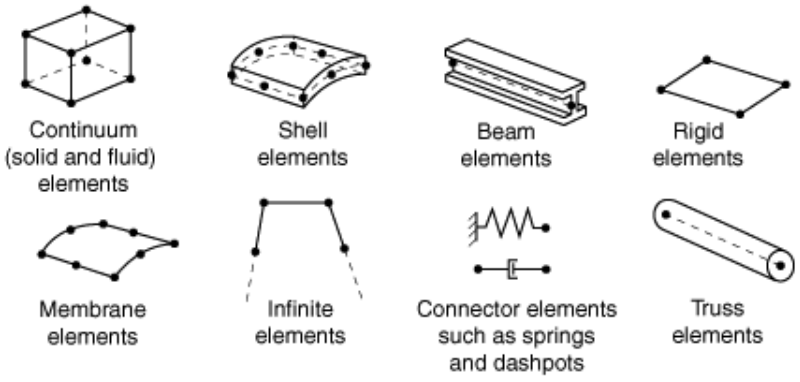

Figure 23: Element families in Abaqus/CAE.

Degrees of freedom is the fundamental variables calculated in each element during analysis and define the element behavior. Different element families are described by different amount of degrees of freedom. For example, shell elements have rotational and translational degrees of freedom, whereas solid elements only have active translational degrees of freedom.

The number of nodes in an element impacts the element's ability to deform and the degrees of freedom. Displacements or other degrees of freedom are calculated at the integration points. At other points in the element, displacements are calculated by interpolation and extrapolation. Elements containing only corner nodes, such as the C3D8 element seen in the top left of figure 23 are calculated with linear interpolation in each direction. These are called linear elements or first-order elements. Elements containing mid-side nodes in addition to the corner nodes are called quadratic elements. They are calculated using quadratic interpolation and are called second-order elements. The total amount of nodes are described in the element name. The 4-node shell element is called S4R, and the 8-node brick element is called C3D8.

An element's formulation refers to the mathematical theory used to define the element's behavior. In Abaqus/CAE, complete generality in material behavior is obtained by using numerical techniques to integrate various quantities over the volume of each element. Gaussian quadrature

is used to evaluate the response in the material in each integration point in each element. Integration options for elements in Abaqus/CAE are reduced or full integration. The integration choice may have a significant effect on the accuracy. Abaqus/CAE uses the letter R at the end of the element name to label reduced-integration elements. For example, C3D8R is the 8-node, reduced-integration, 3D, solid element.

For the two different models, shell and solid elements for the global and local failure models have been used respectively. In the load distribution model shell elements were used, representing a solid model with isotropic stiffness instead of hollow core slabs with different stiffness in the longitudinal and transverse direction. Since the objective of the load distribution analysis is to see how a vertical load is getting distributed in a system of hollow core slabs, and only a linear analysis is done, the magnitude of the load applied to the model does not matter on the distribution of the total force. This is further explained in the following sections.

4.2 Load distribution model

When studying the transverse load distribution, it is important to replicate the shear transfer between the elements. Therefore shear forces in the joint are analyzed. This is because the tensile stresses are only examined for a single hollow core slab in the local failure model, and to simulate a system of slabs, the shear force in the joint is applied to the longitudinal edge of the local failure model. The performed analysis is linear elastic, justified previously in the methodology.

4.2.1 Hollow core system

Based on initial conditions, it makes the most sense to use 3D shell elements, which can provide the most accurate results. Shell elements simplify the shape of a solid element, and when using a shell element there is a difference between thin and thick shells. As described in the article SHELLS vs. SOLIDS [18], thick shells can account for stresses through the element and shear deformations. Thin shells do not account for stress in the direction perpendicular to the surface of the shell. The h/L ratio is important to consider when choosing elements for analysis. A small h/L ratio makes thin shells advantageous because transverse shear is not important, and for a big h/L ratio, solid elements are more advantageous because shear deformation is important to consider. The book Finite Element Analysis Concepts via SolidWorks presents a figure to display element selection based on the h/L ratio [19]:

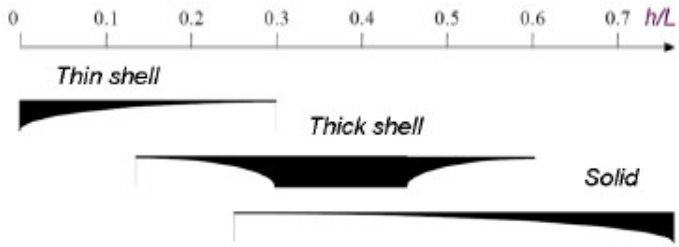

Figure 24: Shell element selection based on h/L ratio.

Hollow core elements can be produced with large spans, usually in the area of 1-20 meters and a height of 200-500mm. Shell elements are also time-saving due to less finite elements when meshing.

The total system consists of five HCS, as mentioned previously, and cast concrete joints. As the joints between the hollow core slabs are non-reinforced and the concrete quality is less than the concrete in the hollow core slabs, it is assumed that longitudinal cracks will be formed in the joints. The joints will therefore be modeled as linear hinges and do not transfer any longitudinal bending moment. This is further explained in the background theory [8][5]. The joints are also modeled using shell elements. The element types for the hollow core slabs are S4R. These are simple quadrilaterals with four nodes, each placed in every corner. It is used reduced integration, which means that the results are calculated from only one integration point.

4.2.2 Materials and orientations

The modeled HCS are 8000x1200mm in the x-y plane, and the joints are 8000x30mm in the x-y plane. The x- and y-directions are shown in figure 25. The material used to describe the shell elements in the model are isotropic C45 concrete. Being isotropic, they have the same material and cross-sectional stiffness in both directions. The concrete in the hollow core slab is modeled with elastic behavior and has a stiffness of 36000 MPa and Poisson's ratio of 0.2. The concrete joints are modeled with C25 concrete as an elastic material using engineering constants. By using user-defined material properties, the material stiffness can be modified in the direction wanted to best model the joints as hinges.

When modifying the material stiffness, the local orientation of each element is important for the behavior. The shell elements were assigned local orientations displayed in figure 25. Understanding the orientations of the elements helps to understand the element behavior when applying forces. The behavior wanted is described in the previously mentioned theory. Two important conditions are zero moments in the support from the moment in the global y-direction because our system is simply supported, and zero moments in the joints from the moment in x-direction caused by the eccentricity of the applied load.

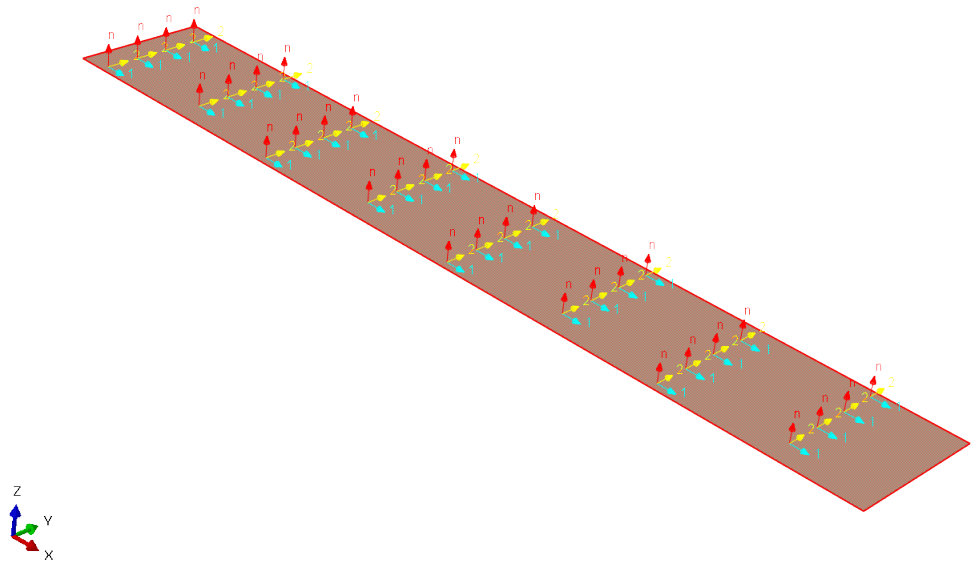

Figure 25: Local material orientation of the modelled shell elements.

Therefore the joints are given a very low stiffness in the transverse direction, E2, because we want to achieve the type of deformation seen in figure 26, below.

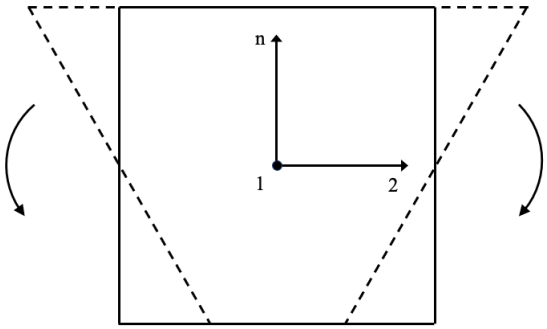

Figure 26: The joint deformation wanted based on local orientation behavior.

The stiffness in the other directions, E1 and E3, is not changed. The low stiffness in the transverse direction makes the transfer of moments along the longitudinal axis insignificant.

4.2.3 Boundary conditions and load

Previous research and information from supervisors have given the necessary background to assume the floor system is supported on concrete or steel beams and not fixed to take moments. The movements in the lateral and horizontal directions are restrained because of the grouted system and the supporting beams. This behavior is represented by restraining the boundary conditions in U2 and U3 on one of the sides and only U3 on the other. This can be seen from figure 27

and 28, where the transverse sides of the HCS are supported. These boundary conditions imply that it should not be any bending moments from rotation about the y-axis in the boundaries. A concentrated load is applied to the edge of the outermost slab with a magnitude of 1 kN to represent the balcony load and easily compute the slabs' load distribution.

4.2.4 Interactions

The constraints between the HCS and the joints are continuous tie constraints. Tie constraints tie two separate surfaces or node regions together to have no relative motion between them. For the shell model in the load distribution analysis, two separate node regions are tied together, even though the default for Abaqus/CAE is using surfaces tied together. [17].

4.2.5 Partitioning and mesh

A simple partition was made to apply the concentrated load at the edge of the slab. Partitions are used to control mesh generation and separate the model into multiple parts. To achieve the concentrated loading on the edge node a partition over the whole system was made. This partition can be seen in figure 27. A mesh seed size of 30 was used on the model.

To obtain the shear forces in the joint for the case where two loads are applied to the same hollow core slab, another partition was made 3000mm from the current partition. The same load of 1kN was also applied here. The partition can be seen in figure 28.

The final result for the two load distribution models is shown in figure 27 and 28.

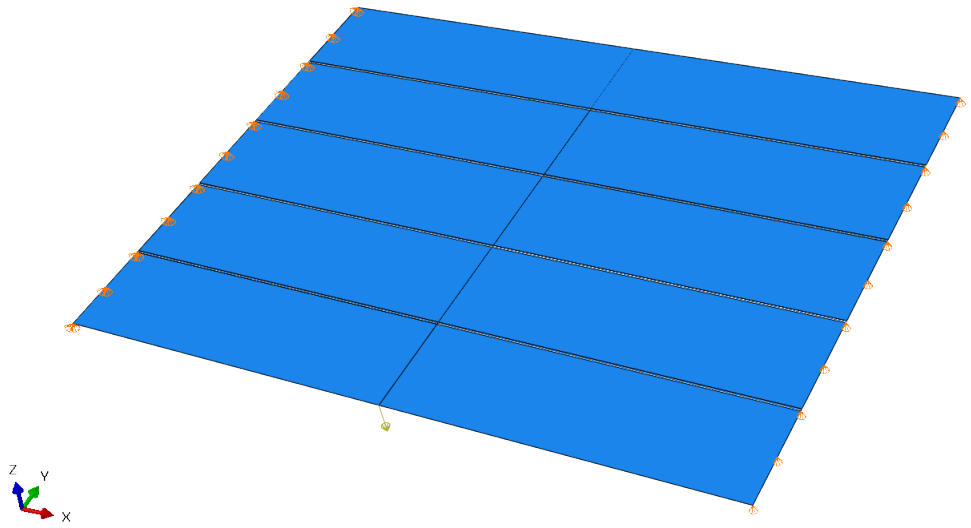

Figure 27: Load distribution model applied one concentrated edge load in the center of the span.

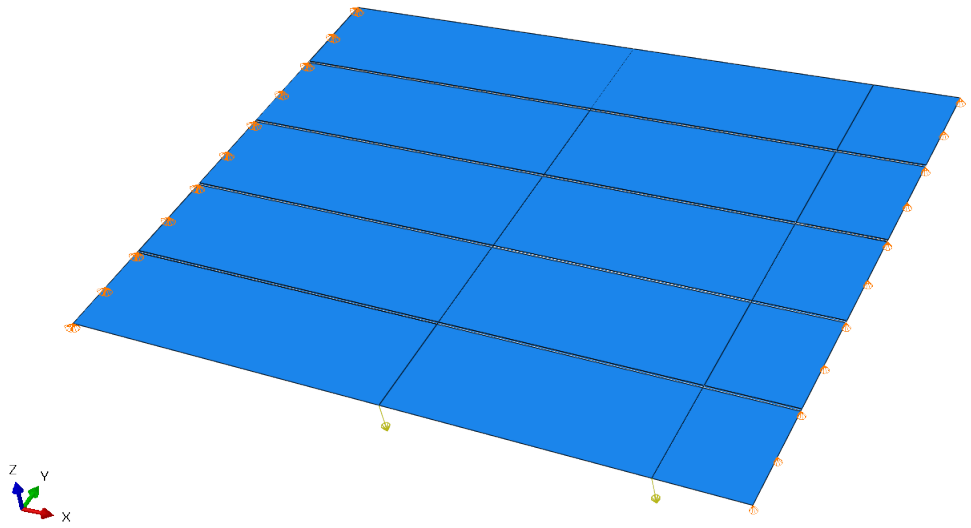

Figure 28: Load distribution model applied two concentrated edge loads, one in the center of the span and one 1000m from the support.

4.3 Local failure model

In reality, the system looks like the one in figure 29. The local failure model is used to analyse tensile stresses in the HCS due to the load situation. So for the local failure model only one slab is modelled to represent the loading situation. This slab is therefore modelled using solid elements, to understand the behavior around the load due to the balcony.

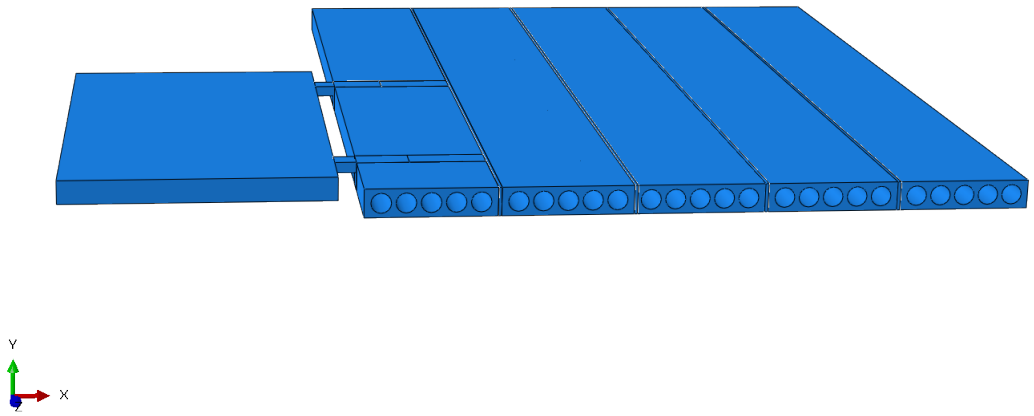

Figure 29: Figure representing the hollow core floor system applied a balcony.

Since the analysis is linear elastic, the principle of superposition can be applied. There are used two different steps for the analysis for the local failure model. These are an initial step for applying the boundary conditions and a load step where the loads are applied. The HCS have been modeled exactly using solid elements without rotating degrees of freedom for the local failure model. Regular C3D8R elements are used for the analysis as these elements are decided to have the best accuracy.

4.3.1 Materials

C45 concrete is used for the entire model. The concrete joint is not modeled, as the local failure model consists of one hollow core slab. The prestressed reinforcement steel has a modulus of elasticity of 195 GPa. The prestressed reinforcement is modelled into the slab, and the steel plate is embedded underneath the area exposed to the loading from the balcony. The steel plate is modeled to represent the connection where the loading from the balcony is transferred to the HCS. In reality, it is common to use an angled steel section, which is welded on top of the steel plate embedded in the concrete, see figure 16. However, modeling the connection exactly is unnecessary when analyzing tensile stresses on the top flange of the HCS. It is assumed that the steel will behave elastically, and the modulus of elasticity is decided to be 210 GPa while the Poisson ratio is decided to be 0.3.

4.3.2 Constraints and boundary conditions

As for the load distribution model, the local failure model is an assembly of several parts. When a hollow core slab is exposed to a permanent, concentrated force, as for this case, the two hollow cores closest to the loading are filled with concrete underneath the area exposed to the loading. To model this the best way, this area is modeled as a solid concrete brick and tied together with the other parts to form the complete hollow core slab. Tie constraints have been used, but in contrast to the load distribution model, tie constraints with a surface-to-surface approach to more accurately model the constraint. Additionally, a steel plate is embedded in the massive concrete part to distribute the concentrated load and increase the capacity against punching shear. The model is simply supported using the same boundary conditions as the load distribution model.

4.3.3 Partitioning and mesh

For this analysis, comprehensive partitioning is done in order to load and mesh the HCS properly. It is desired that the concentrated load works directly into the nodes of the elements and that the pressure load works over entire elements. Partitioning is important so that the load can be applied correctly and so that the mesh will be OK. Additionally, areas of the hollow core slab are not straightforward to mesh correctly. Ideally, the model should be meshed with cube elements with equal lengths. In this model, the challenges arise for the mesh close to the hollow cores. The

partition is done in order to minimize distorted elements in this area.

Additionally, it is important that the mesh in the areas close to the load from the balcony is symmetrical. It is expected to find tension on the top side of the void behind the load, and it needs to be adequately assessed. In the case discussed in this thesis, the tension in the transverse direction is most vulnerable, as cracks on top of the third hollow core can be critical and lead to failure.

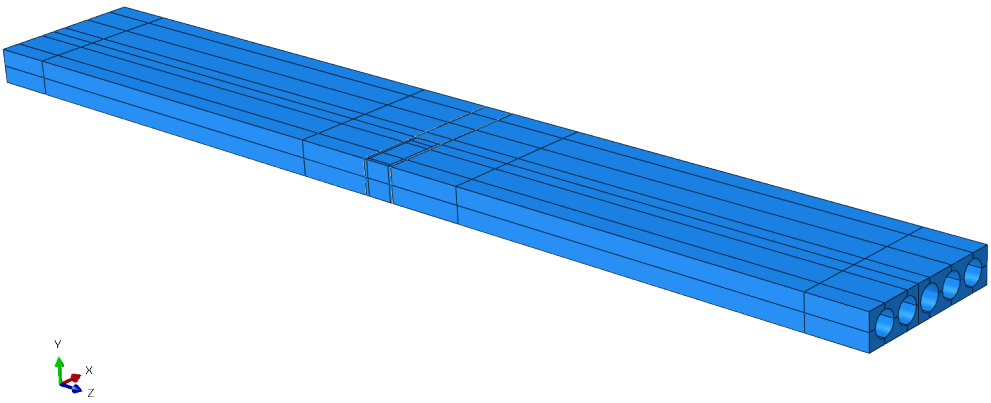

Figure 30: Partition of the local failure model.

4.3.4 Loads applied to the model

The local failure model is exposed to different loads, where the loads from the balconies are the most important. The main contributions of loading are already discussed and calculated in the methodology. There are vertical forces in the connection from the balcony due to the self-weight of the balcony itself and the live load appearing on it. Because the connections have an eccentricity from the vertical load between the balcony and the hollow core slab, a moment can also be transferred. The share of the eccentricity moment dealt with on the hollow core slab depends on the connection between the balcony and the hollow core slab itself. If the connection is completely fixed into the balcony, it is assumed that no moment will be transferred into the hollow core slab. In the opposite case 100% of the moment will be transferred to the hollow core slab if the connection is simply supported in the balcony. It is assumed that for most connections no moment is transferred to the hollow core slab through the connection. Nevertheless, it is of interest in this thesis to look at all the different things that may increase the tensile stresses behind the applied concentrated load. Therefore, the analysis is done for 20%, 50%, and 100% of the eccentricity moment transferred to the hollow core slab, including when no moment is transferred.

Skewed columns and wind may cause significant horizontal loads on the hollow core slab as well, and it is assumed that it is transferred through the connections. Values for the horizontal load are

presented in the methodology. Additionally, the shear forces in the joint, obtained from the results of the load distribution analysis, are used to add a traction force on the edge opposite to the edge connected to the balcony. This is assumed to work uniformly over the entire surface.

Self-weight is also applied to the model as a gravity force working on all parts. The density of concrete is modelled using $2400kg/m^3$ and the density of the steel used in rebars are modelled using $8050kg/m^3$. In the analysis performed in this thesis, the stresses in transverse direction are of interest.

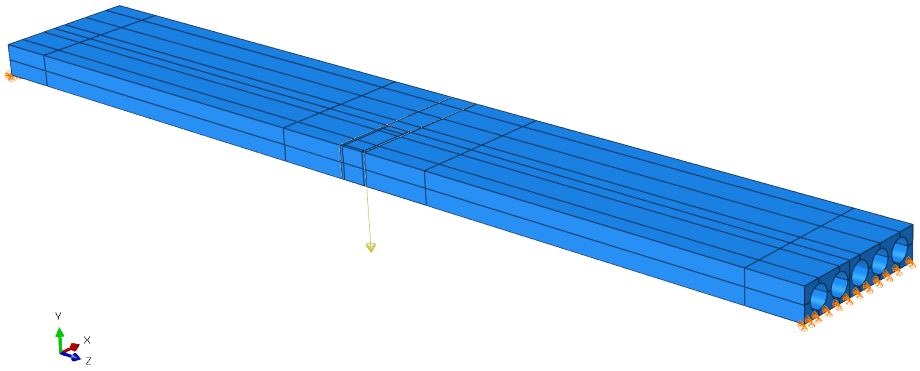

Figure 31: Local failure model applied self weight.

4.3.4.1 Vertical load

The vertical load is distributed over the area of 200x400mm over the steel plate. Using a pressure force distributed over the area, local stresses in the elements under the loading are more realistic than using concentrated loading applied in a single node. The distributed load represents the vertical forces from the balcony transferred to the steel angle and plate cast and welded into the edge of the hollow core slab. The load is shown in figure 32, below.

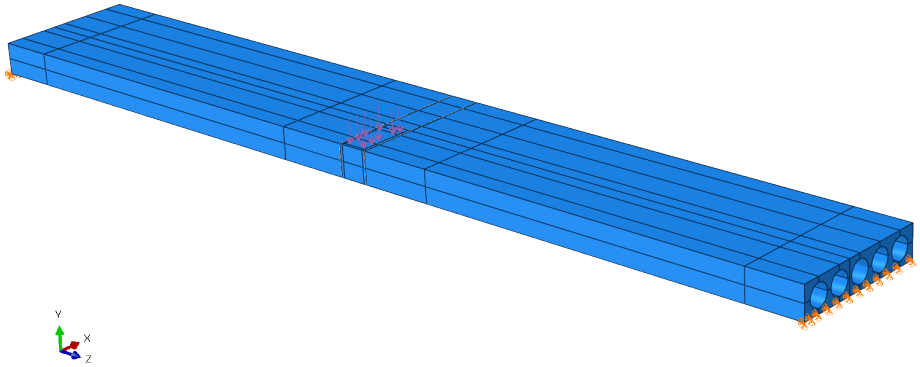

Figure 32: Local failure model applied vertical load.

Figure 33 is the same as the one with center load, but the connection is situated 1000mm from the support.

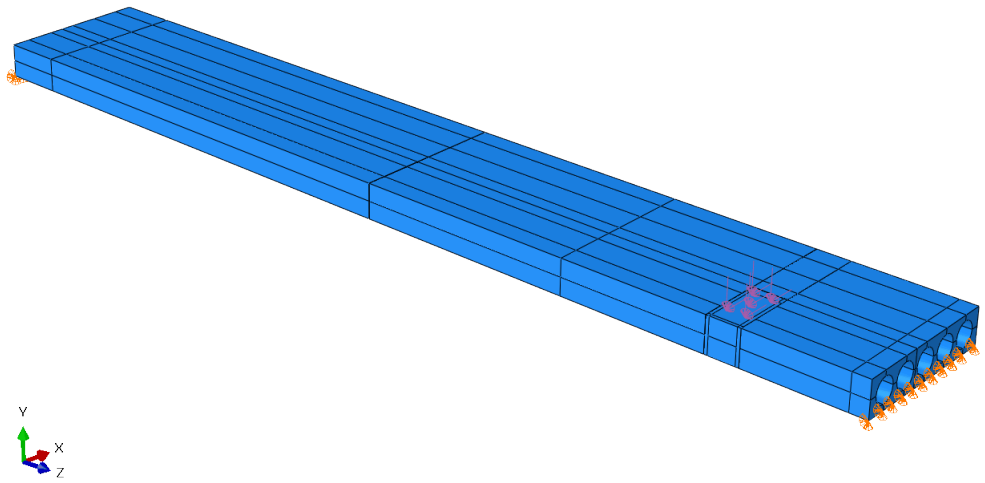

Figure 33: Local failure model loaded 1000mm from the support.

Figure 34 represents the load situation when the slab is applied with two balcony connections. The connections are 3000mm apart. One connection is in the middle of the slab, and the other is 1000mm from the support.

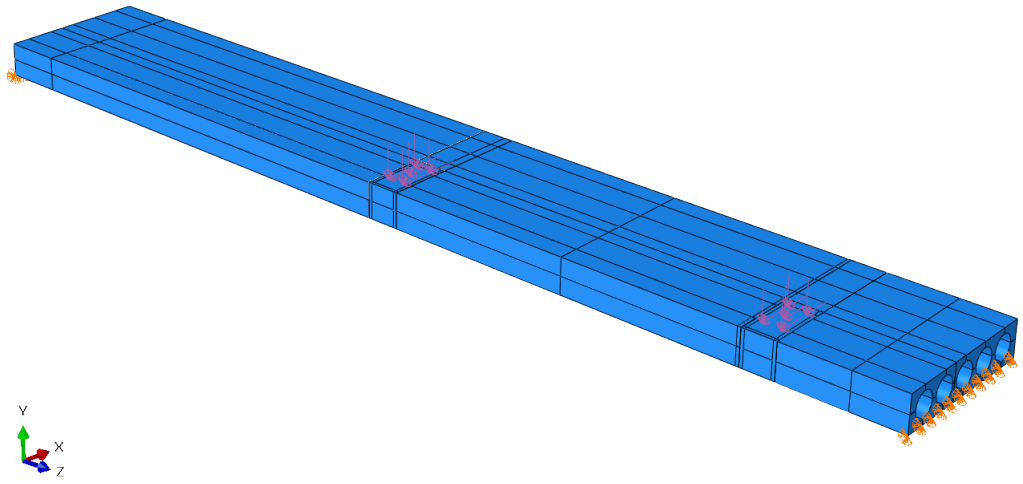

Figure 34: Local failure model loaded in the center of the span, and 1000mm from the support.

4.3.4.2 Horizontal load

The horizontal loading from wind and inclination of the columns under the balcony is applied over the same 200x400mm area as the vertical load. Here, traction load is also used to distribute the horizontal load over an area instead of applying a concentrated load on the edge. A horizontal general traction force over the steel plate area is considered a good representation of this load. The load is shown in figure 35, below.

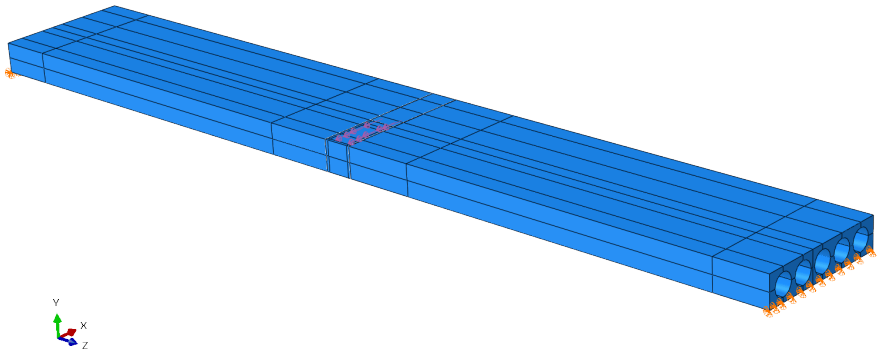

Figure 35: Local failure model applied horizontal load.

4.3.4.3 Eccentricity moment

The moment due to eccentricity of the vertical balcony load is applied on the edge of the hollow core slab. The load is split into two contributions, a pressure load causing tension and one pressure load causing compression in the HCS. Each load is distributed over an area of 132.5x200mm, half the height of the HCS and the width of the balcony to slab connection. This way of applying the moment is the simplest and most efficient way of representing the effect on the HCS without having to model the entire connection and angled steel section. Figure 36 show how the moment is applied.

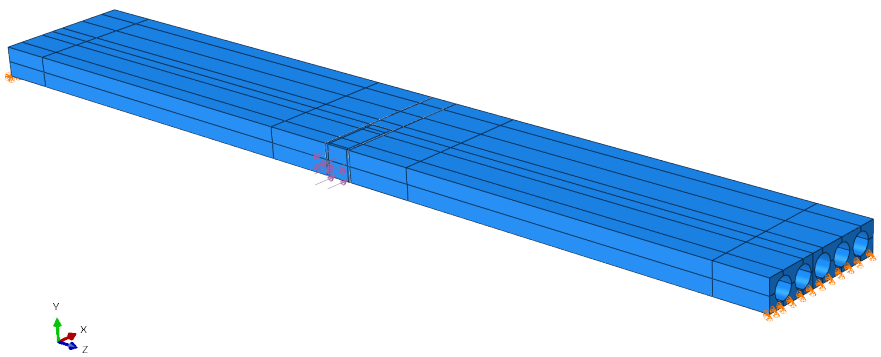

Figure 36: Local failure model applied moment due to eccentricity.

4.3.4.4 Prestressed reinforcement

The prestressed reinforcement is modeled using wire elements embedded into the hollow core section. These are modelled with the distance shown in figure 19, 19, and 19 using a truss section. The element type applied to the reinforcement is T3D2 elements, a 2-node linear displacement element capable of handling axial stresses. The hollow core element and steel reinforcement is applied with an initial temperature of 0 Kelvin. Using the thermal expansion coefficient and strain caused by the prestress, a temperature is calculated in equation (24). This temperature difference causes the strain in the reinforcement, thus simulating prestress. How it looks when applied in the model can be seen in figure 37, below.

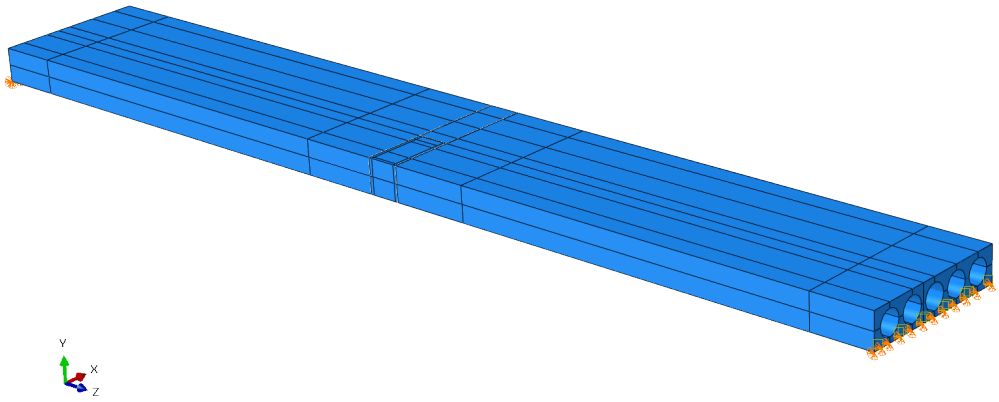

Figure 37: Local failure model applied prestress in the form of temperature strain.

4.3.4.5 Traction forces from load distribution

The shear force in the joint between the first and second hollow core slab is modeled with shear traction forces along the longitudinal edge opposite to the edge exposed to the concentrated loading. Dependent on whether the model is exposed to one or two concentrated loads, the shear force is divided between several loaded areas. For the model exposed to one concentrated load, acting on the edge in the center of the span, the shear force is divided over a total of five areas. Since the loading is symmetric, the two outermost areas are the same size and have the same loading on both sides of the center of the span. In sum, the total traction force applied to this model equals the total shear force in the longitudinal joint obtained from the load distribution model. The same type of distribution of traction forces is done for the model applied with two loads, where the sum of the traction forces over the areas is equal to the shear forces in the joint obtained from the load distribution model with two loads. The application of traction loads can be seen in figure 38.

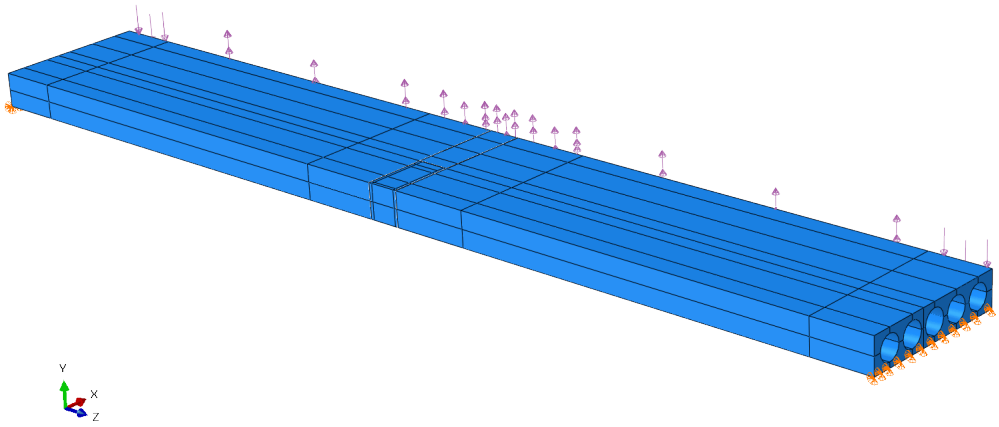

Figure 38: Local failure model applied traction representing load from the rest of the system.

4.3.4.6 Total load situation

The total load situation on the HCS look like this:

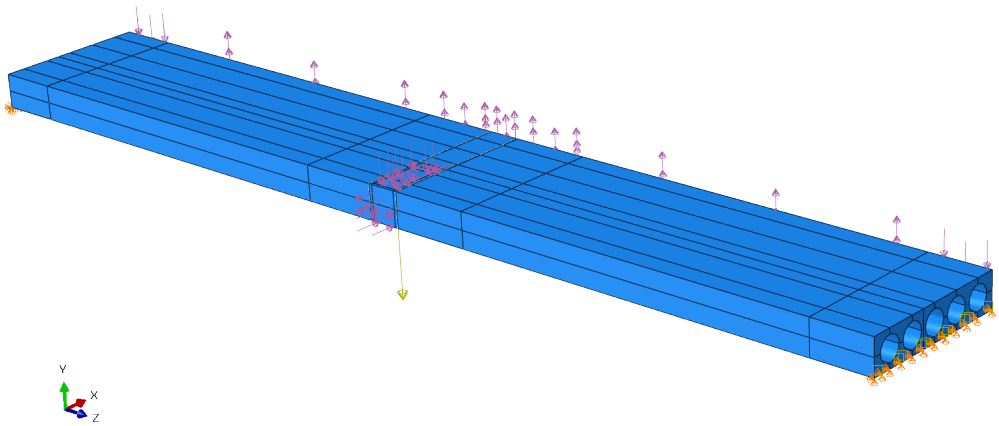

Figure 39: The local failure model applied all the loads presented.

5 Results

The results from both the load distribution model and the local failure model will be presented in the following paragraphs. The analysis of the two problems is done separately, and the results from the load distribution model are used in the analysis of the local failure model. The results will therefore be presented in two different chapters, separate from each other.

5.1 Load distribution model

Analysis of the load distribution in a floor system of hollow core slabs is done, where the outermost slab is exposed to a load in the center of the span, a load 1000mm from the support end, and both of these load situations simultaneously. Results from these analyses are shown in this chapter.

5.1.1 Diagrams from Abaqus/CAE

Figure 40 shows the downward deflection of the system when the outermost slab is exposed to a concentrated edge load in the center of the span. The most deflected area is shown in blue in the diagram.

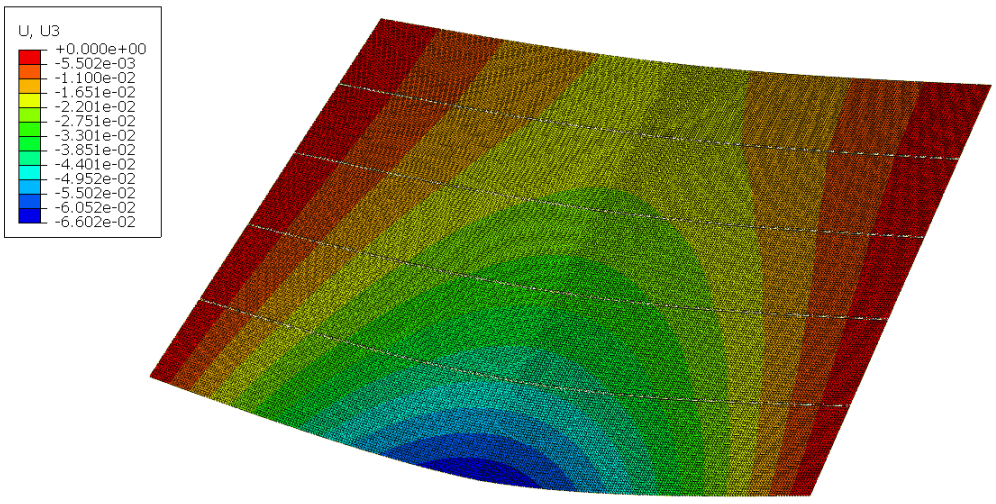

Figure 40: U3 distribution in the load distribution model applied center load.

The figures 41 and 42 show the moment distribution over the slab system. Figure 41 display SM2, which represents bending moment force per unit width about local 1-axis. The local 1-axis for the elements is in the x-direction, showing the moment distribution caused by eccentricity from the applied load. Figure 42 likewise display SM1, representing bending moment force per unit width about local 2-axis. The local 2-axis for the elements are in the y-direction.

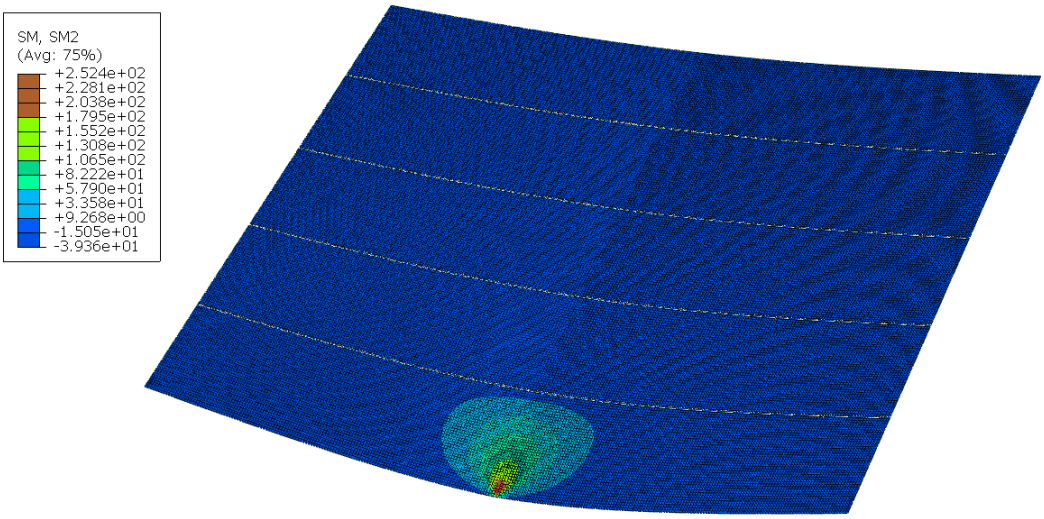

Figure 41: Moment distribution from moment around the longitudinal direction.

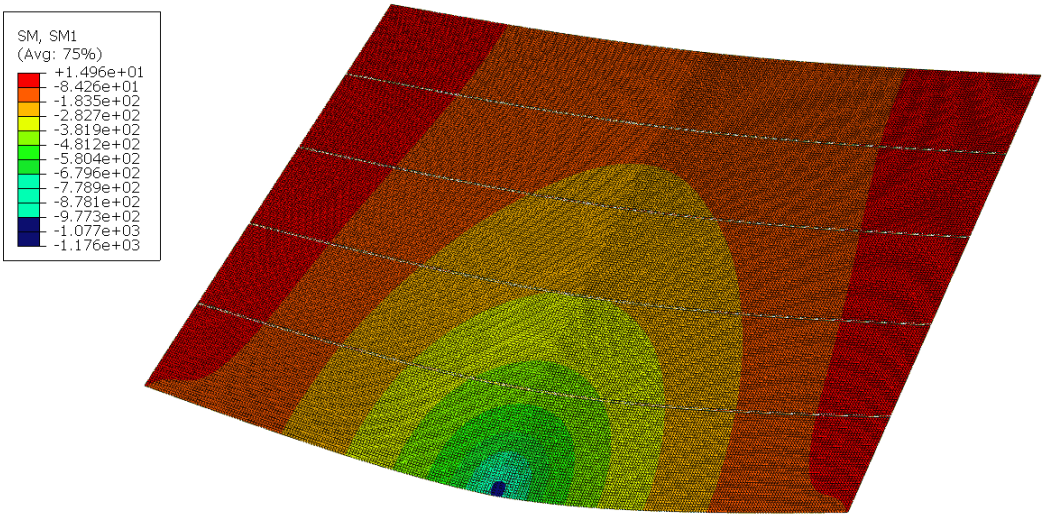

Figure 42: Moment distribution from moment around the transverse direction.

5.1.2 Load distribution factors

The load distribution percentages can be calculated on the basis presented in article [7] or obtained by using the figures already presented from NS-EN 1168 [6]. Table 3 show the calculated load distribution factors for the concentrated load applied at the edge of the first slab. This is done by exporting the U3 and SM1 values in the integration points of each element to excel, and calculating the average displacement and moment in each plate. The load distribution factors are then calculated using the obtained values with equations (1) and (2). They represent how the moment and deflection are distributed in the system of five slabs.

Slab	Deflection ($\mathbf{F}_d$)	Moment ($\mathbf{F}_m$)
1	33.69	33.03
2	23.54	23.53
3	17.32	17.51
4	13.59	13.83
5	11.86	12.09

Table 3: Load distribution factors for moment and deflection.

5.1.3 Shear forces

In order to apply the most accurate joint forces to our local failure model, the shear forces in the joint behind the loaded slab were obtained and analyzed. The job results from Abaqus/CAE with one concentrated edge load provided the shear forces in the transverse direction for the model. By using query and probe values, selecting the elements of interest along the joint, the shear forces could be exported to excel. The shear force distribution in the joint behind the loaded slab was calculated for a situation where the loaded slab was exposed to a concentrated edge load at the center of the span, 1000mm from the supported end, and both simultaneously. This way, the shear forces could be applied to the different local failure models. Diagrams showing the shear force distribution in the joint behind the loaded slab are given below for all the different placements of the vertical load.

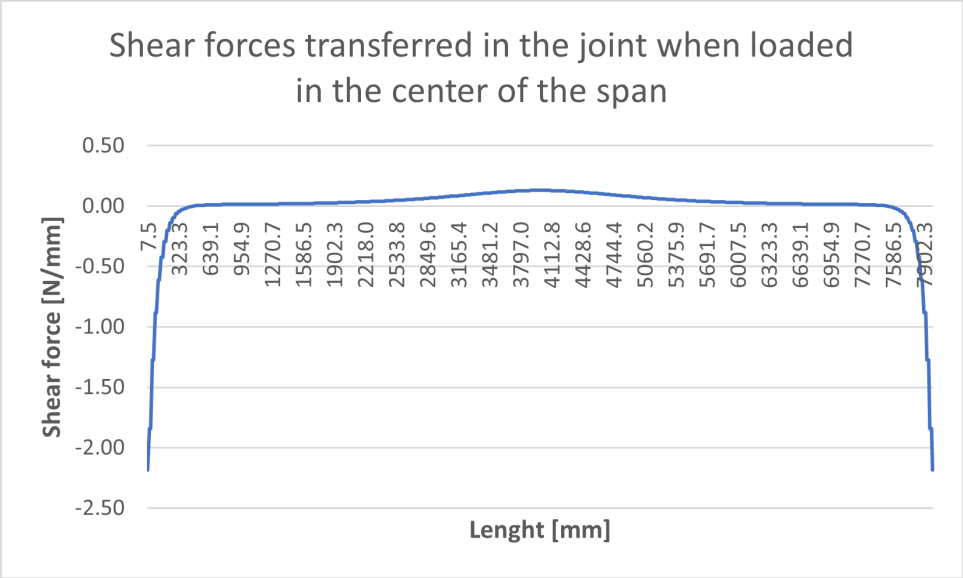

Figure 43: Shear forces in the first joint when the outermost slab is loaded in the center of the span.

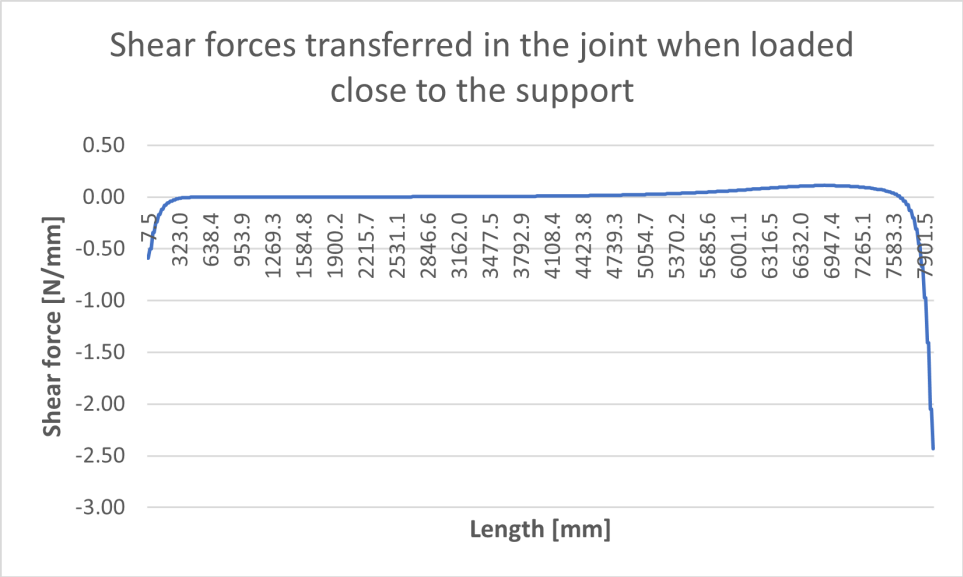

Figure 44: Shear forces in the first joint when the outermost slab is loaded 1000mm from the support.

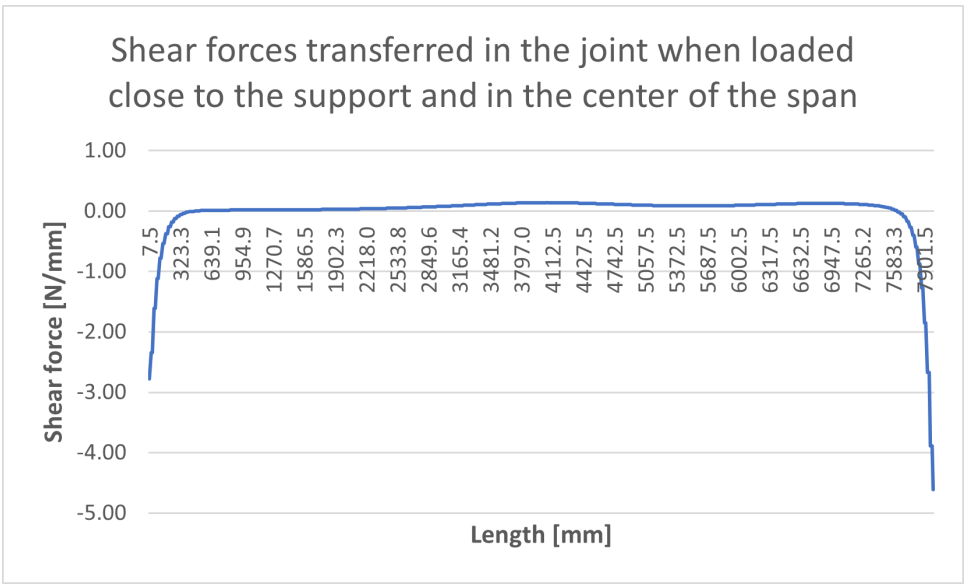

Figure 45: Shear forces in the first joint when the outermost slab is loaded in the center of the span and 1000mm from the support.

5.1.4 Reaction forces and concentrated forces in the corners

Figure 46 shows the reaction forces in the z-direction distributed in the boundaries over the width of the system. The vertical lines illustrate the edge of concrete joints where the joint and plate share a node. Looking at these resulting reaction forces in the boundaries, the first slab is the most loaded and withstands over 100% of the total load.

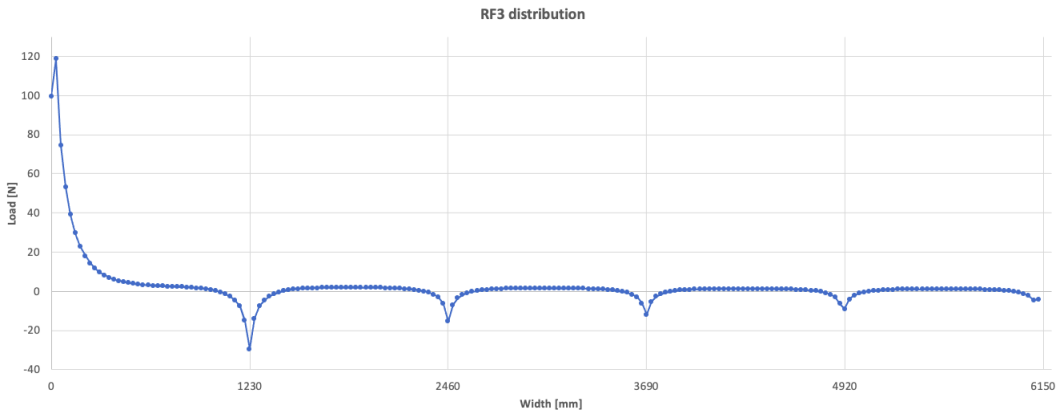

Figure 46: Distribution of vertical forces in the boundaries over the width of the system.

In the corners, where the joints meet the boundary condition on the transverse edge of the slabs, large tensile forces appear in the supports in addition to sizeable negative shear transfer in the joint. The shear forces are not uniform along the width of the joint, as seen from figure 43. The total shear forces in the joint add up to the total reaction forces in the first plate minus the applied load, showing that the system is in static equilibrium.

5.2 Local failure model

The local failure model is used to analyze the capacity against concentrated edge loading of HCS. The capacity is analyzed concerning the tensile stresses developing on the top side of the void behind the load in the slab, where analysis show is the worst place as seen from figure 47. This area is further referred to as the critical area.

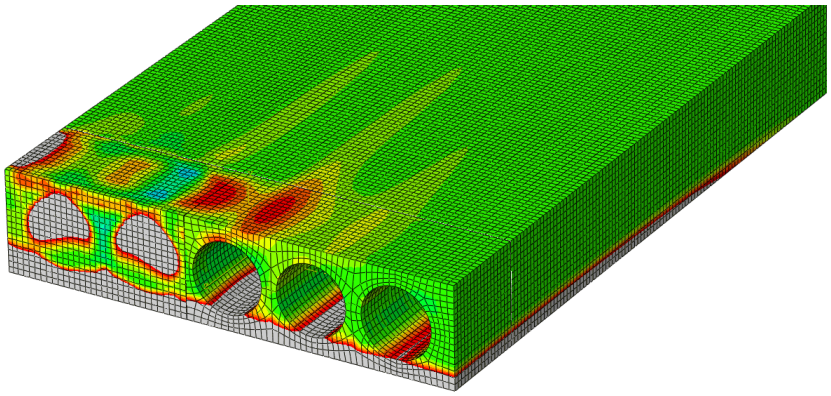

Figure 47: The critical area over the void behind the concentrated load where the tensile stresses are obtained, colored in deep red.

In order to find the most significant tensile stresses present, principal stresses are evaluated in the analysis. Figure 47 shows the area with the highest tensile stresses and how the tensile forces

spread out over the void.

Three different HCS are analyzed in Abaqus/CAE. The span is kept constant at 8000mm, and the different HCS analyzed are 200mm, 265mm, and 320mm in height. All of the slabs are analyzed with two different load situations. The first one being only one concentrated load acting in the center of the span, and the other situation is concentrated loading applied 1000mm from the edge. The center distance between the two load situations is 3000mm. Areas over the voids behind the load are most vulnerable to tensile failure, and the tensile forces are therefore presented in the tables below. The displacements, U, are also reported for the slabs with center load, to see how they are affected by the parameter variation.

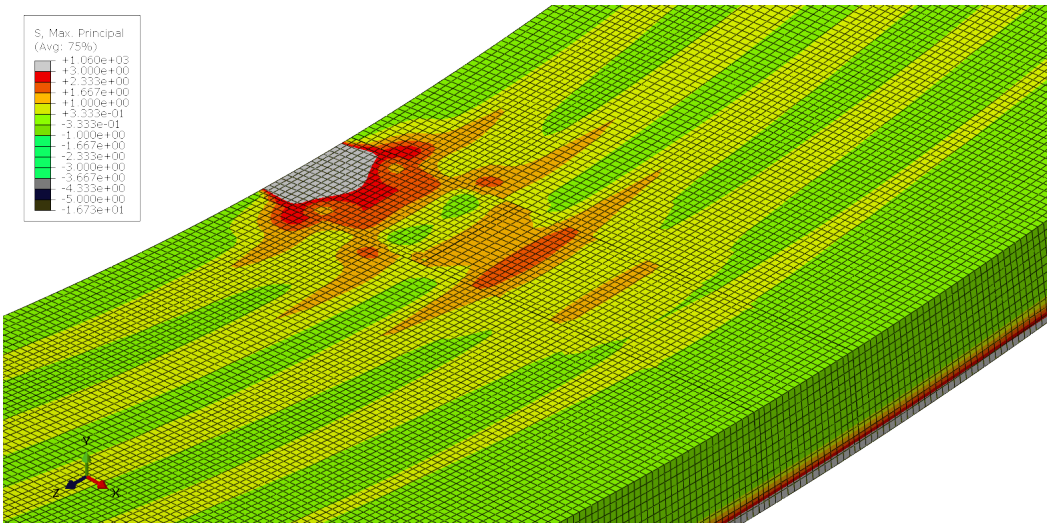

Figure 48: Areas with high tensile forces in the top of the HCS, center load.

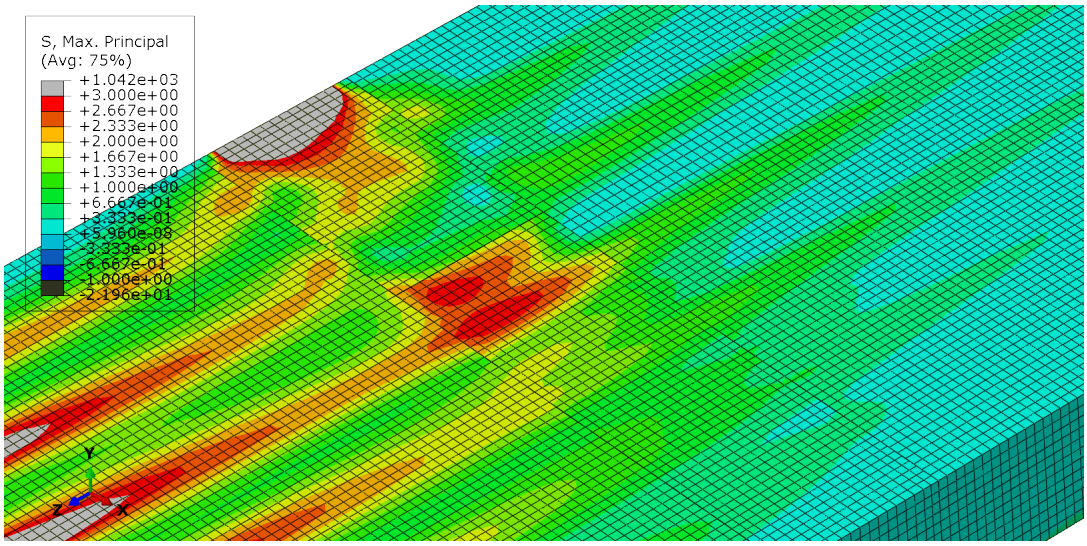

Figure 49: Areas with high tensile forces in the top of the HCS, load 1000mm from support.

5.2.1 Principal stresses

In this section, the results from the analysis done with different loading conditions are shown. Some parameters stay constant. All the analysis is performed with the maximum amount of reinforcement bars and the depth of the steel plate being constant at 20mm below the surface of the hollow core slab. All the results show HCS exposed to a single concentrated load. Results from analysis varying the parameters mentioned above will be presented in the following chapters. The tables presented in this chapter will be with the 200mm, 265mm, and 320mm HCS varying the applied vertical and horizontal load from the balcony, in addition to different amounts of eccentricity moment. More information about the applied loads is given in the load chapter in the methodology, and how they are applied to the model is shown in the finite element modeling chapter.

Type	Vertical load [kN]	Horizontal load [kN]	Moment [%]	U [mm]	Max principal stress [MPa]	$\left[\frac{\sigma_{max}}{f_{ctd}}\right]$
200mm HCS	59.1	7.3	100	17.54	2.49	1.63
			50	17.24	2.14	1.40
			20	17.07	1.93	1.26
			0	16.95	1.78	1.16
	59.1	3.0	100	17.52	2.40	1.57
			50	17.23	2.05	1.34
			20	17.06	1.84	1.20
			0	16.94	1.70	1.11
	30.3	4.2	100	10.91	1.35	0.88
			50	10.77	1.16	0.76
			20	10.68	1.06	0.70
			0	10.61	0.99	0.65
	30.3	1.7	100	10.91	1.30	0.85
			50	10.76	1.11	0.73
			20	10.67	1.00	0.72
			0	10.61	0.93	0.61

Table 4: Values for 200mm HCS, center load.

Type	Vertical load [kN]	Horizontal load [kN]	Moment [%]	U [mm]	Max principal stress [MPa]	$\left[\frac{\sigma_{max}}{f_{ctd}}\right]$
265mm HCS	59.1	7.3	100	7.14	1.08	0.70
			50	7.02	0.97	0.64
			20	6.94	0.89	0.58
			0	6.89	0.85	0.56
	59.1	3.0	100	7.13	1.04	0.68
			50	7.01	0.93	0.61
			20	6.94	0.86	0.56
			0	6.89	0.81	0.53
	30.3	4.2	100	4.55	0.61	0.40
			50	4.49	0.55	0.36
			20	4.45	0.52	0.34
			0	4.43	0.49	0.32
	30.3	1.7	100	4.55	0.59	0.38
			50	4.49	0.53	0.35
			20	4.45	0.49	0.32
			0	4.42	0.47	0.31

Table 5: Values for 265mm HCS, center load.

Type	Vertical load [kN]	Horizontal load [kN]	Moment [%]	U [mm]	Max principal stress [MPa]	$\left[\frac{\sigma_{max}}{f_{ctd}}\right]$
320mm HCS	59.1	7.3	100	4.33	0.59	0.39
			50	4.25	0.58	0.38
			20	4.20	0.56	0.37
			0	4.17	0.55	0.36
	59.1	3.0	100	4.32	0.58	0.38
			50	4.25	0.56	0.37
			20	4.20	0.55	0.36
			0	4.17	0.54	0.35
	30.3	4.2	100	2.76	0.35	0.23
			50	2.72	0.33	0.22
			20	2.69	0.32	0.21
			0	2.68	0.32	0.21
	30.3	1.7	100	2.75	0.34	0.22
			50	2.72	0.33	0.22
			20	2.69	0.32	0.21
			0	2.67	0.31	0.20

Table 6: Values for 320mm HCS, center load.

Type	Vertical load [kN]	Horizontal load [kN]	Moment [%]	Max principal stress [MPa]	$\left[\frac{\sigma_{max}}{f_{ctd}}\right]$
200mm HCS	59.1	7.3	100	3.00	1.96
			50	2.54	1.66
			20	2.27	1.48
			0	2.09	1.37
	59.1	3.0	100	2.89	1.89
			50	2.43	1.59
			20	2.16	1.41
			0	1.98	1.29
	30.3	4.2	100	1.59	1.04
			50	1.38	0.90
			20	1.25	0.82
			0	1.16	0.76
	30.3	1.7	100	1.53	1.00
			50	1.32	0.86
			20	1.19	0.78
			0	1.10	0.72

Table 7: Values for 200mm HCS, loaded 1000mm from the support.

Type	Vertical load [kN]	Horizontal load [kN]	Moment [%]	Max principal stress [MPa]	$\left[\frac{\sigma_{max}}{f_{ctd}}\right]$
265mm HCS	59.1	7.3	100	1.39	0.91
			50	1.23	0.80
			20	1.14	0.75
			0	1.08	0.71
	59.1	3.0	100	1.34	0.88
			50	1.18	0.77
			20	1.09	0.71
			0	1.04	0.68
	30.3	4.2	100	0.80	0.52
			50	0.75	0.49
			20	0.69	0.45
			0	0.66	0.43
	30.3	1.7	100	0.78	0.51
			50	0.70	0.46
			20	0.66	0.43
			0	0.63	0.41

Table 8: Values for 265mm HCS, loaded 1000mm from the support.

Type	Vertical load [kN]	Horizontal load [kN]	Moment [%]	Max principal stress [MPa]	$\left[\frac{\sigma_{max}}{f_{ctd}}\right]$
320mm HCS	59.1	7.3	100	1.26	0.82
			50	0.98	0.64
			20	0.81	0.53
			0	0.71	0.46
	59.1	3.0	100	1.19	0.78
			50	0.90	0.59
			20	0.73	0.48
			0	0.69	0.45
	30.3	4.2	100	0.86	0.56
			50	0.71	0.46
			20	0.63	0.41
			0	0.57	0.37
	30.3	1.7	100	0.81	0.53
			50	0.67	0.44
			20	0.58	0.38
			0	0.52	0.34

Table 9: Values for 320mm HCS, loaded 1000mm from the support.

The results indicate that the 200mm HCS are most vulnerable for failure under concentrated edge loading. Especially with loading close to the support. For all the HCS, regardless of the height, the principal tensile stresses are largest for the cases where the loading is applied 1000mm close to the support.

5.2.2 Variation in the number of reinforcement bars

In order to figure out whether the number of reinforcement bars used in the HCS affects the tensile stresses in the critical area, different amount of reinforcement bars are used in the analysis. For the 265mm HCS, the maximum amount of reinforcement bars used are 10. Additionally, 8, 7, and 4 bars are analyzed. The analysis is also performed to see whether a non-symmetric distribution of the reinforcement bars impacts the tensile stresses appearing behind the load. In this case, 10, 8, and 4 bars represent a symmetric distribution of the bars, while 7 bars represent a non-symmetric distribution. The different HCS have been analyzed with a general load case. General load case will be used for elements analyzed with a vertical load of 59.1kN, a horizontal load of 3.0kN, and no eccentricity moments.

Type	Vertical load [kN]	Horizontal load [kN]	Load Placement	Number of bars	Max principal stress [MPa]
265mm HCS	59.1	3.0	Center	10	0.81
				8	0.80
				7	0.79
				4	0.76
			Edge	10	1.07
				8	1.05
				7	0.96
				4	0.93

Table 10: Principal tensile stresses in the critical area for different number of reinforcement bars.

5.2.3 Effect of two loads on one hollow core slab

There may be a need to place both of the balcony supports on a single hollow core slab. This may affect the tensile stresses developing around the concentrated load. The stresses have been examined in the center of the span, in the critical area, and close to the slab's support in the critical area. The results are given in the table below.

Height	Vertical load [kN]	Horizontal load [kN]	Stresses behind the edge load [MPa]	Stresses behind the center load [MPa]
200mm	59.1	3.0	2.91	1.76
265mm	59.1	3.0	1.52	0.87
320mm	59.1	3.0	1.04	0.57

Table 11: Change in tensile stresses in the critical area caused by two loads on the hollow core slab.

5.2.4 Steel plate placement

Another variation is how deep the steel plate is placed under the concentrated load. In all the cases and analyses, the steel plate is placed 20mm below the concentrated load, and the concentrated load is applied on an area equal to the area of the steel plate. In the results given below, analyses are done with the steel plate placed on the same level as the top side of the HCS and right in the middle of the slab. The slabs are analyzed with the general load case.

Height	Vertical load [kN]	Horizontal load [kN]	20mm depth	0mm depth	Placed in the middle
200mm	59.1	3.0	1.70	1.63	1.59
265mm	59.1	3.0	0.81	0.79	0.80
320mm	59.1	3.0	0.54	0.56	0.58

Table 12: Change in tensile stresses in the critical area caused by the placement of the steel plate.

5.2.5 Numerical errors

Analyses have been performed on the 265mm HCS to figure out the effect the change in mesh size has on the results for the principal stresses in the critical area. For most of the results presented earlier, a mesh size of 15mm has been used, so analyses on both a 10mm mesh and a 30mm mesh have been performed on the case with the general load case applied on the 265mm HCS. Results are given in the table below.

Height	Vertical load[kN]	Horizontal load [kN]	10mm mesh size [MPa]	15mm mesh size [MPa]	30mm mesh size [MPa]
265mm	59.1	3.0	0.84	0.81	0.71

Table 13: Values for principal stresses in the critical area of the 265mm HCS slab with center load for different mesh sizes.

6 Capacity control

The maximum force applied to the different HCS with respect to the tensile capacity of the concrete is not analyzed in this thesis. However, the tensile stresses have been analyzed, taking into account loads from two different balconies. With these results, the critical force applied to the HCS before reaching the tensile capacity is calculated by linearizing the applied vertical load with the utilization factor to find the vertical load corresponding to a utilization factor of 1. The minimum and maximum critical force for the 200mm HCS with high applied horizontal load are calculated by the use of results from table 7. The calculations are done as followed:

$$\frac{59.1kN}{1.37} = 43.1kN$$

$$\frac{30.3kN}{0.76} = 39.9kN$$

These calculations are done for all the three HCS with both high and low horizontal applied load. The vertical loads calculated is the one that give tensile stresses in the critical area behind the applied load equal to the tensile strength of the concrete. This is done for both of the vertical loads from the balconies in figure 17 and 18, creating a span of vertical capacities where the critical load will lie within. The span is given in table 14, below. The vertical capacities are calculated with 0% eccentricity moment transferred to the HCS.

The HCS capacity against punching shear is calculated with equation 6. The capacity control is done for a concentrated load distributed over two of the webs, in this case for the two outermost webs. Although the thickness of the outermost web is a bit thicker, the thickness of the inner web is used as a conservative assumption for the calculations of the capacity for punching shear. The heights used in the equation are found in figure 13, 14 and, 15. Additionally, the α value is assumed to be 1, $f_{ctd} = 1.53$ MPa shown in table 1, and the $\sigma_{cp} = 4$ MPa.

Type	Cap. for punching shear	Applied hor. load	ecc. moment	Min. critical force	Max. critical force
200mm HCS	76.2 kN	High	0%	39.9 kN	43.1 kN
		Low	0%	42.1 kN	45.8 kN
265mm HCS	115.4 kN	High	0%	70.5 kN	83.2 kN
		Low	0%	73.9 kN	86.9 kN
320mm HCS	174.1 kN	High	0%	81.9 kN	128.8 kN
		Low	0%	89.1 kN	131.3 kN

Table 14: Results from capacity control of punching shear.

7 Discussion

7.1 Load distribution model

The behavior of the load distribution model are presented in figure 40, 41 and, 42. According to the initial behavior assumptions, the distribution provided in figure 41 and 42, show that the joints transfer no longitudinal moment (dark blue color), and the supports transfer no transverse moments (dark red color). The results represent the model behavior wanted, proving that the choices made in Abaqus/CAE are applied correctly. The deformation of the joint presented in figure 26 in the finite element modeling chapter shows the joint behaving like a hinge in Abaqus/CAE, as wanted, and figure 41 confirms this behavior.

The load distribution factors in table 3 show an almost identical percentage of distribution as recommended in diagram C.3 in Annex C in NS-EN 1168 [6], without adding the 1.25% addition when there is no structural topping on the first slab subjected to the concentrated edge load. The first slab shows a load distribution factor of 33.03 % compared to 33.3 % read from figure 4. The results are only varying by 1-2 percent compared to the Eurocode solution. This means that the model accurately represents the load distribution effect in a system of HCS. The results verify the initial problem statement of understanding and verifying the load distribution model presented by Betongelementforeningen.

The analysis follows recommendations from NS-EN 1168, saying that the elements should be assumed to be anisotropic or isotropic. Although HCS are made with concrete, an isotropic material, HCS have an anisotropic stiffness due to the reinforcement and longitudinal voids in only one direction. However, the model is a simple shell model, and the analysis is assumed good enough when assuming elements with isotropic stiffness.

The results obtained from the analyses show that the resultant force from the shear forces in the joint is working downward on the loaded hollow core slab. The reason is that the forces close to the corners both in the joint and in the supports are preventing the corners to move upwards. Figure 43 and 46 shows this result and the relationship between shear and the vertical reaction forces. They also show the spike of forces in the corners of the plate. Large shear forces close to the support contribute to the resultant force in the shear transfer and push the first hollow core slab downward. This is most likely caused by the mechanical behavior of the system, caused by the restraint against upward deflection of the slab mentioned earlier. The sum of all obtained reaction forces over the entire system adds up to precisely 1kN, which was applied, and shows that the system is in equilibrium.

7.2 Local failure model

Presented in the results are the highest tensile stresses in the critical area of the different HCS seen in figure 48 and 49 with only center loading, only loading 1000mm the support, and both at the same time. Since the HCS is reinforced in the longitudinal direction, the amount of tension the slab can resist in the transverse direction solely depends on the concrete's tensile capacity. From figure 49 and 48, it can be seen that the highest values for tensile stresses in the concrete occur in the critical area for center load and load 1000mm from the support. The highest principal stresses in the critical area depend on the stresses in the longitudinal direction. The higher the stresses are in the longitudinal direction, the higher the principal stresses are, which is analyzed in this thesis.

7.2.1 Balcony size

The two balconies chosen are presented in the methodology in figure 17 and 18. The largest balcony is used to simulate a force equal to the vertical capacity of the connection. Some connections may resist a higher vertical load, thus supporting even larger balconies causing loads over 60kN. The size of the balcony may also affect the center distance between two connections. In some cases, two connections will be put on the same hollow core slab, and the distance between them impacts each other's stresses. Larger balconies also affect both the horizontal and vertical forces applied to the connection. The wind load, however, may be affected more significantly as the wind area may become larger. Variation in the height of the railing will also affect the horizontal load transferred to the HCS. Increasing the vertical load will directly increase the moment caused by eccentricity if it is transferred.

7.2.2 Vertical load

The vertical load is calculated from the self-weight of the two different balconies with their respective live loads. Increase in the applied vertical load increase the tensile stresses in the critical area. For the 265mm HCS, the tensile stresses in the critical area increase from 0.47MPa to 0.81MPa when the vertical load is applied to the center of the span and is increased from 30.3kN to 59.1kN. This is an increase in tensile stresses of 72.3%. For the situation where the load is applied close to the slab's support, the increase in tensile stresses is 65.1% due to the load increase. The tensile stresses in the critical area behind the edge load are still much higher than for the load applied in the center of the span. For the general load case, the max principal stress is 1.04MPa when the load is applied to close to the slab's support, an increase of 28.4%.

For the 200mm HCS, the tensile stresses increase by 82.8% when the load is placed in the center of the span and by 80.0% when the load is placed close to the slab support due to the increase in vertical load. For the 320mm HCS, the tensile stresses increase by 74.2% when the load is applied

in the center and by 32.7% when the load is applied close to the slab's support. The change in vertical forces also affects the eccentricity moment, causing even more increased tensile stresses if transferred. The vertical forces are limited by the vertical capacity of the connection, the HCS capacity, and the shear capacity of the joints. The vertical forces need to be handled with caution not to cause failure when applied.

7.2.3 Horizontal load

The slab is analyzed with two different horizontal loads. The largest load is due to wind loads from Bodø, where the design wind speed is 30m/s, and the lower horizontal load is due to wind load from Oslo. The speeds are according to the NA in EC1 [**Fotnote**]. Horizontal loads have an impact on the tensile stresses observed in the critical area. Differences in the results are caused by the change of horizontal forces applied and the type of HCS analyzed. For the HCS with a thickness of 320mm applied with a center load, the difference between the two horizontal loads is almost negligible, varying from 0.54MPa to 0.55MPa when increasing the horizontal load from the general load case to 7.3kN. For the loads placed close to the support, tensile stresses vary more, from 0.69MPa to 0.71MPa, when the horizontal load increases from the general load case to 7.3kN. For the load cases where a larger portion of the eccentricity moment is transferred to the HCS, the tensile stresses increase a lot more for an increasing horizontal load. When 20% of the eccentricity moment is transferred, there is an increase from 0.73MPa to 0.81MPa when the horizontal load increases from 3.0kN to 7.3kN. The same applies to other values for the transferred moment. When the transferred moment is 50% the increase in the tensile stresses is 0.08MPa and when all of the moment is transferred the tensile stresses increases by 0.07MPa. The trend, however, is that when the slab is loaded in the center of the span, the increase in tensile stresses due to increased applied horizontal load will be larger for thinner slabs. When the load is applied close to the slab's support, the tensile stresses will increase equally for all the slabs.

7.2.4 Effect of prestressing and variation in number of tendons

The tensile stresses close to the support are significantly higher than the stresses due to the load being placed in the center of the span. A reason for this is that the prestress and the self-weight of the concrete make the tensile stresses large in the longitudinal direction close to the support, but in the center of the span, the tensile stresses are replaced with large compression stresses. When the longitudinal stresses are in tension, they affect the principal stresses and make them larger. Originally, the prestress will work on the hollow core slab uniformly and give the same longitudinal stresses everywhere on top of the hollow core slab. The gravity, however, works more in the center of the span to overcome the tensile stresses developed by the prestress. The impact from the gravity will be lower on the tensile stresses to a cut closer to the support because of a shorter moment arm to the gravity force. For the general load case, the increase in tensile stresses

from the case where the concentrated load is applied in the center of the span to the case where the load is applied close to the support of the slab is 16.5% for the 200mm HCS, 28.4% for the 265mm HCS and 27.8% for the 320mm HCS.

Seen in table 10, the principal stresses in the critical area are not subjected to significant changes when varying the number of reinforcement bars. When the HCS are loaded with the general load case in the center of the span, the tensile stresses are reduced from 0.81MPa to 0.76MPa when reducing prestressed tendons from 10 to 4. That is a reduction of 6.2%. When the slab is loaded close to the support of the edge, the reduction for the 265mm HCS with the general load case is 13.1%. This is a reduction from 1.07MPa to 0.93MPa. The distribution of the reinforcement is symmetric for the three cases where the number of bars is in even numbers. If the HCS has 7 reinforcement bars embedded, the reinforcement is non-symmetric in the slab. There was believed that non-symmetric reinforcement would affect the tensile stresses in the critical area, but there are no clear signs of that in the results. The principal stresses in the critical area are gradually reducing when the number of reinforcement bars is reduced.

7.2.5 Eccentricity moment & connection detail

The results indicate that the moment has a significant impact on the tensile stresses in the critical area, see figure 48 and 49. In the product description, Invisible Connections imply that the connection does not transfer any moment, caused by the eccentricity of the balcony loading. If these forces are transferred, important tensile and compressive forces are transferred directly into the HCS, giving stresses capable of reaching the concrete tensile capacity. Comparing the values in table 7, 100% moment transfer to 0% moment transfer causes an increase in tensile stresses of nearly 0.90 MPa for large vertical and horizontal loads. With a tensile capacity of 1.53 MPa, this increase can lead to cracks in the critical area and should be avoided.

The moment is transferred to the hollow core slab from the balcony because of the eccentricity length and how the connection is detailed. In the analysis performed in this thesis, the eccentricity length is 200mm. If the connection is fixed in the balcony, no moment will be transferred to the hollow core slab. Ideally, the balcony will take most of the moment, but in some cases, the moment will be transferred to the hollow core slab. Dependent on the HCS, an increased moment will greatly impact the tensile stresses appearing in the critical area. For the load applied close to the slab's support, 100% moment transfer will cause the max principal stresses to exceed the tensile strength of the concrete for the 200mm HCS, load with 30.3kN, with either the high or low horizontal load applied. When applying a maximum value for the eccentricity moment to the general load case for the 265mm HCS loaded in the center of the span, the tensile stresses will be 28.4% larger, from 0.81MPa to 1.04MPa. For the case where the load is applied close to the support, the tensile stresses are 28.8% larger with 100% moment transfer. There is also important that if the connection is completely fixed to the balcony and simply supported on the hollow core

slab, the balcony must resist the moments. The moment will be larger if the eccentricity length increases or is lower if the eccentricity length decreases. In this task, the eccentricity length is modeled as the distance between the balcony slab and the hollow core slab.

7.2.6 Effect of one vs. two balcony connections on one hollow core slab

As seen from the results, in table 11, the tensile stresses increase by 3.5 % to 7.4 % behind the center load when two connections are applied to the same slab. However, behind the load applied close to the support, tensile stresses increase more. Here, the increase in tensile stresses are 47.0% for the stresses on the 200mm HCS, 46.2 % for the 265mm HCS, and 50.7 % for the 320mm HCS. The two applied loads cause a severe increase in the tensile stresses in the critical area behind the load applied close to the slab's support. In other words, the analysis shows that the HCS can not withstand the same concentrated forces if two forces are applied to a single hollow core slab. The tensile stresses may be 50% larger in the critical area, depending on the placement of the load. There is reason to believe, due to the results, that the tensile stresses could be more severe behind the load close to the support if this load is placed closer to the support than 1000mm. The same can be said if the load placed in the center of the span is placed closer to the same support as the other load. In these cases, the tensile stresses in the most severe places could be more than 50% larger.

7.2.7 Placement of the steel plate

The regular placement of the steel plate is 20mm below the surface of the hollow core slab and 25mm from the longitudinal edge. To see the effect the placement of the steel plate has on the tensile stresses, analyses with 0mm of concrete coverage and h/2 concrete coverage were done. From table 12, the results show that the 265mm HCS and the 320mm HCS does not get affected a lot by the placement of the steel plate. The 200mm HCS, however, show clear signs that the tensile stresses are larger when the steel plate is placed in its regular position while the stresses are lower both for the situation where the plate is placed in the middle and when the plate is placed in the top of the slab. When the steel plate is placed in the middle, the tensile stresses are 6.5 % smaller than the stresses for the regular case.

7.2.8 Capacity control of punching shear and the use of different types of HCS

The control of punching shear is done according to Betongelementboken Bind C, chapter 3.1.2.5. The calculations show that the punching shear capacity is higher than the capacity for concentrated load when the tensile stresses in the critical area are investigated. Compared to the maximum critical force, when the slab is applied with the low horizontal load, the capacity for punching shear is 66.4% larger for the 200mm HCS. For the same load case, for the 265mm HCS, the

maximum capacity for punching shear is 33.1% higher than the maximum critical force from the analysis. For the 320mm HCS, the same capacity control is done, and the capacity for punching shear is 32.6% higher. Although the capacity against the concentrated load applied to the edge of the hollow core slab has a large span for the 320mm HCS, the capacity for punching shear is always higher than the obtained vertical load capacity. Therefore the vertical load capacity limits the concentrated edge load due to the tensile stresses in the critical area.

Figure 1 show common slab types used in the industry in Norway. The 265mm HCS analyzed in this thesis are similar to the 265mm HCS with circular voids displayed in the figure, although the width of the element analyzed is 1200mm. The void's diameter for the 200mm HCS used in the analysis, shown in figure 13, is in the upper limit of the shown diameter range. The diameter of the void in the element analyzed is 154mm, while the range from the figure varies from 140mm to 155mm. The large diameter causes the flange in the top of the slab to be small, causing higher tensile stresses in this area. For the 320mm HCS, the cross-section is adjusted seen in figure 15, in order to make modeling and analysis easier. Instead of non-circular voids displayed in the figure 1, circular voids are modeled in the hollow core slab. Comparison between the two cross-sections shows that the height of the non-circular in both of the 320mm HCS in figure 1 is higher than the void diameter in the 320mm HCS modeled. This leads to the opposite problem of what appears in the 200mm HCS. The thickness of the flange is usually thinner in reality than the thickness of the flange used in the analysis. This may result in the analysis showing too small tensile stresses. The reason for not using non-circular voids in the modeled cross-section is the danger of shear failure in the webs due to the non-varying thickness of the web over a certain height.

The capacity against concentrated loads without reinforcing the loaded slab with the steel plate is not controlled because the connection detail is always assumed to include the steel plate. The capacity against end anchorage failure is also not calculated because the capacities calculated in the already mentioned table C12.7 in Bind C [8] are always larger than the applied horizontal load.

7.2.9 Sources of error

There will be some numeric errors linked to the choice of partition and element type. However, in the end, the analysis was performed with small elements, so the numeric errors should be negligible. There is still reason to assume some numerical errors in the model. The analysis is run with a mesh size of 15mm, and tests have been done with different mesh sizes on the 265mm hollow core slab with a load applied to the center of the span. In addition to the analysis with the 15mm mesh, analyses have been performed with a mesh size of 10mm and 30mm to determine the analyses' numerical error. The difference in the calculated principal stresses are large for the mesh with a size of 15mm to a size of 30mm with a difference of 12.3 %. When the analysis was run with a mesh size of 10mm, the stresses were 3.7 % larger. With these results in mind, the stresses will become larger with a smaller mesh size than those used in these analyses. Although the most significant

leap occurs when the mesh is reduced from 30mm to 15mm, there is still reason to believe that the appearing stresses are larger in reality than what has been analyzed in these analyses. The reason why the analyses have not been performed with a smaller mesh than 15mm is mainly because of computational time. However, the results are believed to be not far from correct, but maybe a safety factor should be multiplied to cope with the numerical error related to mesh size.

Installation of the balcony to HCS connection is usually done manually, either on a construction site or by the HCS manufacturer. This is done by chipping out the concrete where the connection is to be placed. This causes a different base situation for each slab due to the tiny differences in execution. When casting concrete around the connection and in the chipped out part of the HCS, there may be areas subjected to bonding weakness causing moment transfer from the connection where it is not recommended. Controlling these weaknesses is very difficult without taking the structure apart after the slabs are placed and loaded. In most cases, no problems arise related to failure or damage in the HCS caused by the manual installation, but it is necessary to consider if the connections are designed close to their capacity. As seen from the presented results, moments cause the most significant increase in tensile stresses in the top face of the slab, hence being unwanted during installation.

The longitudinal stresses are getting bigger and bigger when moving closer to the support, regardless of the placement of the concentrated load. This may not be realistic because the reinforcement is not modeled with an anchorage length. In the analyses, the reinforced bars have a uniform temperature field across the length, which simulates a uniform prestress throughout the length of the structure. When it comes to the anchorage length, this assumption is not entirely valid, because the prestress will have a length to develop in the concrete. In this analysis, the prestress will work from the first mm of the slab. Since the self-weight of the concrete slab is small close to the support, only the prestress will work in the longitudinal direction, and the tensile stresses will be large, especially over the hollow cores. Therefore, the concentrated loads are not applied any closer than 1000mm from the support of the hollow core slab because of the incorrect tensile stresses appearing on the top side of the slab due to the short anchorage length. There can be seen that the principal tensile stresses are highest when the concentrated loads are placed close to the support. Therefore, if concentrated loads are planned to be applied even closer than 1000mm away from the support, additional analyses should be performed to see if the tensile stresses are below the critical limit. Transmission length, anchorage length, and bond stresses are calculated in Appendix B.

8 Conclusion and future work

8.1 Conclusion

Analyses were done on a floor system of hollow core slabs to see how the forces were distributed when the outermost slab was exposed to a concentrated edge load. Additionally, analyses on a single hollow core slab were performed to figure out the resulting tensile stresses in the different HCS due to the concentrated edge loads. Different parameters were varied to see how they affected the tensile stresses over the void behind the concentrated edge load. Both of the problems were analyzed in Abaqus/CAE.

The results show that the outermost slab distributes the highest share of the total moment deflection from the load distribution analysis. 33.69 % of the total deflection and 33.03 % of the total moment are in the loaded slab. The distribution of the deflection and moment in the other slabs are given in the table below. When it comes to the support forces, more than the applied concentrated edge load is supported on the first slab. In figure 43, 44, and 45, the load distribution of shear forces in the joint can be seen for the different load cases. There are large negative values for the shear forces in the joint close to the supports, which give rise to the total shear force in the joint being negative, pushing the loaded slab down.

Slab	**Deflection ($\mathbf{F}_d$)**	**Moment ($\mathbf{F}_m$)**
1	33.69	33.03
2	23.54	23.53
3	17.32	17.51
4	13.59	13.83
5	11.86	12.09

The local failure model is analyzed with a general load case with a vertical load of 59.1kN, a horizontal load of 3.0kN, and the maximum number of reinforcement bars. It can be observed that the 320mm HCS has the best safety margin against tensile failure, while the 200mm HCS struggle with large loads. Generally, higher vertical and horizontal loads cause higher tensile stresses in the critical area. With the general load case applied in the center of the 200mm HCS, the tensile stresses reach well over the tensile strength of the concrete, independently of the horizontal load and the eccentricity moment applied. The stresses obtained are 1.70MPa in the critical area. This is 11.1% higher than the tensile strength. The 200mm HCS subjected to loading 1000mm from support experience increased tensile stresses compared to the center loading. For the general load case with no moment transfer, the tensile stresses are 1.98 MPa, which is 29.4% above the tensile strength. Additionally, the tensile strength is reached when a vertical load of 30.3kN is applied, regardless of the applied horizontal load, when 100% of the eccentricity moment transferred.

When it comes to the 265mm and the 320mm HCS, they can resist higher concentrated loads. The general load case for the 265mm HCS gives tensile stresses of 0.81 MPa with no moment transfer when the slab is exposed to a concentrated edge load in the center of the span. This is 47.1% below the tensile strength. When the load is applied 1000mm from the support, with the same loading conditions, the tensile stresses are 1.04 MPa. This is 32.0% below the tensile strength. The stresses for the 320mm HCS are even lower.

The variations of prestressed strands in the HCS do not affect the tensile stresses in the critical area significantly for the general load case. The maximum principal stresses vary from 0.76 MPa to 0.81 MPa when the number of bars varies from 4 to 10. When the load is applied close to the support, the difference is larger, varying from 0.93 MPa to 1.07 MPa (table 10). The tensile stresses in the critical region are not affected by the non-symmetric placement of the bars. The placement of the steel plate does not affect the tensile stresses significantly, thus not being a critical factor for capacity design (table 12). Lastly, the effect of two concentrated edge loads applied to the same HCS causes tensile stresses behind the load close to the support to increase by 47% for the 200mm HCS, 46.2% for the 265mm HCS, and 50.7% for the 320mm HCS compared to the single load counterpart. Behind the center load, on the other hand, the tensile stresses increase from 3.5% to 7.4% (table 11).

The capacity against punching shear was calculated and compared to the results from the Abaqus/CAE analysis. The comparison shows that the linearized HCS capacity against concentrated edge loads limits the punching shear capacity. The maximum capacity for punching shear is 66.4% larger for the 200mm HCS, 33.1% larger for the 265mm HCS, and 32.6% larger for the 320mm HCS compared to the linearized vertical load values (table 14).

8.2 Future work

Future work includes exactly modeling the entire slab system with the balcony to slab connection making accurate load tables for specific connections. If stress states in a particular case need to be evaluated, a non-linear approach may be necessary.

For the 200mm HCS element where the tensile stresses are beyond the tensile capacity, it may be a possibility to fill three hollow cores with concrete instead of two. These suggestions are not researched in this thesis but can be interesting to examine. The results suggest the tensile stresses one can expect in the top flange of the HCS but do not evaluate the total capacity.

Additionally, a study can be done on the variation of the flange thickness, as the flange thickness itself might have a more considerable influence on the tensile stresses than the variation of the cross-section height. The length of the cast concrete in the outermost hollow cores may be varied to see its effect on the tensile stresses.

Bibliography

[1] Standard Norge (2018) *NS-EN 1992-1-1:2004+A1:2014+NA:2018: Eurocode 2: Design of concrete structures - Part 1-1: General rules and rules for buildings.* Available at: https://www.standard.no/no/Nettbutikk/produktkatalogen/Produktpresentasjon/?ProductID=997272 (Accessed: 17. March 2021).

[2] MAKLADA, *PC STRAND TECHNICAL DATA* Available at: http://www.maklada.com/upload/1390038767.pdf (Accessed: June 10, 2021)

[3] Betongelementforeningen (2010) *Betongelementboken bind A Bygging med betongelementer*, 4th edition

[4] FIP technical paper (1984) *Transversal distribution of linear loadings in prestressed hollow core floors*

[5] Telford, T. (1988) *Precast prestressed hollow core floors, FIP techincal paper*

[6] Standard Norge (2012) *NS-EN 1168:2005+A3:2011: Precast concrete products - Hollow core slabs.* Available at: https://www.standard.no/no/Nettbutikk/produktkatalogen/Produktpresentasjon/?ProductID=511314 (Accessed: 01. February 2021).

[7] Elliott, K. S, Song, J. and Kwak, H. (2009) *Load distribution factors for hollow core slabs with in-situ reinforced concrete joints, International Journal of Concrete Structures and Materials Vol.3, pp. 63 69.*

[8] Betongelementforeningen (2013) *Betongelementboken bind C Elementer og knutepunkter*, 4th edition

[9] Walraven, J.C. and Mercx, W.P.M. (1983) *The Bearing Capacity of Prestressed Hollow Core Slabs*

[10] Broo, H. Lundgren, K. and Engström, B. (2005) *Shear and torsion interaction in prestressed hollow core units, Magazine of Concrete Research 57(9):521-533.* ,

[11] Derkowski, W. (2015) *Torsion of precast hollow core slabs, Cracow University of Technology.*

[12] FIP Bulletin No. 06 (2000), *Special design considerations*

[13] Aswas, A and Jacques, F. J. (1992) *Behavior of Hollow-Core Slabs Subjected To Edge Loads*

[14] Pajari, M. (2005) *Resistance of prestressed hollow core slabs against web shear failure, VTT RESEARCH NOTES 2292.*

[15] Standard Norge (2016) *NS-EN 1990:2002+A1:2005+NA:2016: Eurocode: Basis of structural design.* Available at:

https://www.standard.no/no/Nettbutikk/produktkatalogen/Produktpresentasjon/?ProductID=814830 (Accessed: 19. May 2021).

[16] Standard Norge (2009) *NS-EN 1991-1-4:2005+NA:2009 Eurocode 1: Actions on structures - Part 1-4: General actions - Wind actions.* Available at: https://www.standard.no/no/Nettbutikk/produktkatalogen/Produktpresentasjon/?ProductID=398860 (Accessed: April 18, 2021).

[17] Dassault systems simulia (2011) *Abaqus 6.11, Abaqus/CAE User's Manual*

[18] Kuusisto, E *E SHELLS vs. SOLIDS — Finite Element Analysis Quick Review*, July 22, 2017

[19] Akin, J. E. (2009) *Finite Element Analysis Concepts: via SolidWorks* 1st edition

[20] Sørensen, S.I. (2013) *Betongkonstruksjoner* 2nd edition, Tapir Akademiske Forlag.

[21] Formelsamling TKT4220 Betongkonstruksjoner 2. NTNU: Institutt for Konstruksjonsteknikk; 2010.

Appendix

A Transfer of prestress

EC2-1-1 point 8.10.2

8.10.2.2(1): [1] At release of tendons, the prestress may be assumed to be transferred to the concrete by a constant bond stress:

$$f_{bpt} = \eta_{p1}\eta_1 f_{ctd}(t) \tag{25}$$

$\eta_{p1} = 3.2$ for 7-wire strands

$\eta_1 = 1.0$ for good bond conditions

$f_{ctd}(t) = \alpha_{ct} \cdot f_{ctk,0,05}/\gamma_c = 0.85 \cdot 2.7MPa/1.5 = 1.53MPa$

$f_{bpt} = \eta_{p1}\eta_1 f_{ctd}(t) = 4.90MPa$

8.10.2.2(2): The basic value of the transmission length:

$$l_{pt} = \alpha_1\alpha_2\phi\sigma_{pm0}/f_{bpt} \tag{26}$$

$\alpha_1 = 1.0$ for gradual release

$\alpha_1 = 1.25$ for sudden release

$\alpha_2 = 0.19$ for 7-wire strands

$\phi = 12.9$mm which is the nominal diameter of tendon

$\sigma_{pm0} = P_0/A = 103.2kN/100mm^2 = 1032MPa$ which is the tendon stress just after release

$l_{pt} = \alpha_1\alpha_2\phi\sigma_{pm0}/f_{bpt} = 516mm$ for tendons with gradual release $l_{pt} = \alpha_1\alpha_2\phi\sigma_{pm0}/f_{bpt} = 645mm$ for tendons with sudden release

The design value of the transmission length should be taken as the less favourable of the two values: $l_{pt1} = 0.8l_{pt}$ when controlling local stresses at release $l_{pt2} = 1.2l_{pt}$ when controlling the ultimate limit state

8.10.2.3: Anchorage of tensile force for the ultimate limit state Bond strength for anchorage:

$$f_{bpd} = \eta_{p2}\eta_1 f_{ctd} \tag{27}$$

$\eta_{p2} = 1.2$ for 7-wire strands

$\eta_1 = 1.0$ for good bond conditions

$f_{ctd} = \alpha_{ctd} f_{ctk,0,05}/\gamma_c = 1.53MPa$

$f_{bpd} = \eta_{p2}\eta_1 f_{ctd} = 1.836MPa$

8.10.2.3(4): The total anchorage length for anchoring a tendon:

$$l_{bpd} = l_{pt2} + \alpha_2\phi(\sigma_{pd} - \sigma_{pm0})/f_{bpd} = l_{pt2} + (F_{pd} - P_\infty)/(\pi \cdot \emptyset \cdot f_{bpd}) = l_{pt2} + l_{pt3} \tag{28}$$

$F_{pd} = f_{p0,1k} \cdot A = (1640MPa/1.15) \cdot 100mm^2 = 142.7kN$

$P = 0.85 \cdot 103.2kN = 87.7kN$ Prestress force, reduced for 15% loss

$F_{pd} - P = 142.7 - 87.7 = 55kN$

$l_{p2} = 1.2 \cdot l_{pt}$

$l_{p2} = 619mm$ for gradual release

$l_{p2} = 774mm$ for sudden release

$l_{pt3} = (F_{pd} - P_{\infty})/(\pi \cdot Ø \cdot f_{bpd}) = 739mm$

$l_{bpd} = l_{p2} + l_{p3}$

$l_{bpd} = 1358mm$ for gradual release

$l_{bpd} = 1513mm$ for sudden release

B Prestress information

To accurately model the prestress reinforcement common values was given from a contact in the concrete industry. The given values are used by a Norwegian manufacturer in production of hollow core slabs. This information is also available from the prestress manufacturer Maklada, in their MAKLADA PC STRAND TECHNICAL DATA [2], under Uncoated Strand 7-Steel Wire for Prestressed concrete EN 10138 - 3:March 2011.

Kvalitet Y1860S7, nr 1.1366

12,9mm spenntau	-A_s = 100 mm²/tau (nominelt) (Ebjelke d_{ekv} = 11,284 mm)	
	-Bruddlast (char. max. force)	-F_m = 186 kN/tau
	-0,1% strekkgrense (proof force)	-$F_{p0,1k}$ = 164 kN/tau

Figure 50: Properties of the reinforcement used for prestressing

C Examples of possible solutions

In cooperation with invisible connections who makes connections between hollow core elements and balconies some common solutions are presented. By understanding the behavior of the connections the load situation and application can be defined.

The most common option from invisible connections is to two BWC-connectors on each hollow core element. BWC stands for balcony wall connector. Their connections have a maximum vertical capacity of 55-60 kN and a horizontal capacity of 20kN. The connector use a support with a steel angle attached to the HCS as shown in the figure below. A steel plate is cast into the hollow core element, and a steel angle is welded on top to distribute the load.

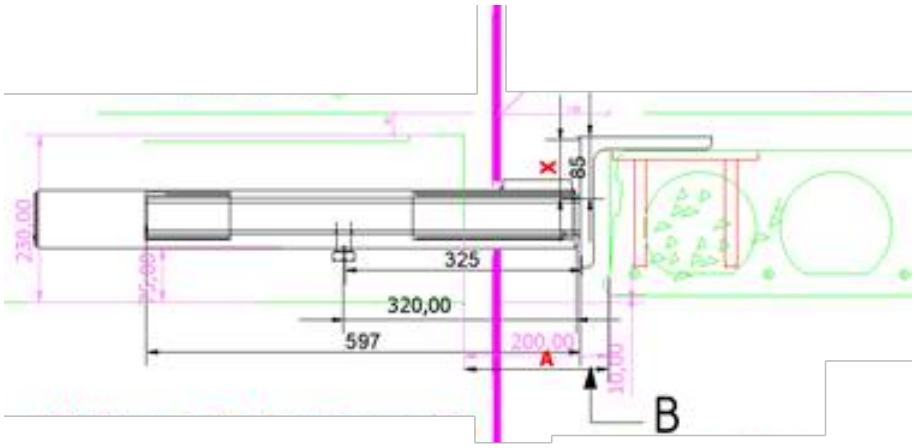

Figure 51: BWC 55

Another possibility is to use the option BWC 55 light, which has a slightly different load situation. The outer pipe is welded to the plate on top or cast into the hollow core element.

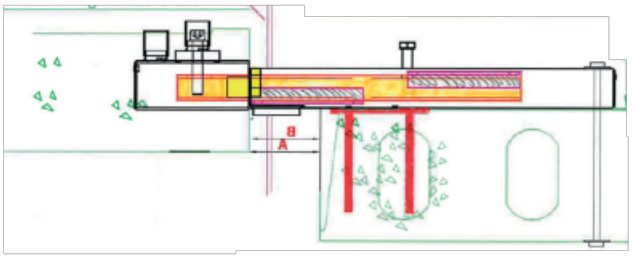

Figure 52: BWC 55 light

Common for all the connections designed by invisible connections is that the moment due to eccentricity of the loaded point is not transferred from the connection to the HCS. The moment is dealt with by the concrete balcony.

D Loads applied the finite element model

D.1 Traction loads for center loaded slabs

Type	Vertical load [kN]	Applied traction load [MPa]	Area applied [mm]
200mm HCS	30.3	-8.28E-02	0mm - 376mm
		5.16E-03	376mm - 3278mm
		1.81E-2	3278mm - 4722mm
		5.16E-03	4722mm - 7624mm
		-8.28E-02	7624mm - 8000mm
	59.1	-1.61E-01	0mm - 376mm
		1.01E-02	376mm - 3278mm
		3.52E-02	3278mm - 4722mm
		1.01E-02	4722mm - 7624mm
		-1.61E-01	7624mm - 8000mm

Type	Vertical load [kN]	Applied traction load [MPa]	Area applied [mm]
265mm HCS	30.3	-5.17E-02	0mm - 466mm
		4.07E-03	466mm - 3278mm
		1.34E-02	3278mm - 4722mm
		4.07E-03	4722mm - 7533mm
		-5.17E-02	7533mm - 8000mm
	59.1	-1.01E-01	0mm - 466mm
		7.94E-03	466mm - 3278mm
		2.62E-02	3278mm - 4722mm
		7.94E-03	4722mm - 7533mm
		-1.01E-01	7533mm - 8000mm

Type	Vertical load [kN]	Applied traction load [MPa]	Area applied [mm]
320mm HCS	30.3	-3.87E-02	0mm - 526mm
		3.42E-03	526mm - 3248mm
		1.09E-02	3248mm - 4752mm
		3.42E-03	4752mm - 7474mm
		-3.87E-02	7474mm - 8000mm
	59.1	-7.55E-02	0mm - 526mm
		6.67E-03	526mm - 3248mm
		2.12E-02	3248mm - 4752mm
		6.67E-03	4752mm - 7474mm
		-7.55E-02	7474mm - 8000mm

D.2 Traction loads for slabs loaded 1000mm from the support's end

Type	Vertical load	Applied traction load [MPa]	Area applied [mm]
200mm HCS	30.3	-2.06E-02	0mm - 406mm
		2.23E-03	406mm - 6219mm
		1.38E-02	6219mm - 7712mm
		-1.18E-01	7712mm - 8000mm
	59.1	-4.02E-02	0mm - 406mm
		4.35E-03	406mm - 6219mm
		2.69E-02	6219mm - 7712mm
		-2.29E-01	7712mm - 8000mm

Type	Vertical load	Applied traction load [MPa]	Area applied [mm]
265mm HCS	30.3	-1.32E-02	0mm - 496mm
		1.73E-03	496mm - 6219mm
		1.05E-02	6219mm - 7652mm
		-7.48E-02	7652mm - 8000mm
	59.1	-2.57E-02	0mm - 496mm
		3.37E-03	496mm - 6219mm
		2.05E-02	6219mm - 7652mm
		-1.46E-01	7652mm - 8000mm

Type	Vertical load	Applied traction load [MPa]	Area applied [mm]
320mm HCS	30.3	-1.36E-02	0mm - 556mm
		1.46E-03	556mm - 6219mm
		8.66E-03	6219mm - 7621mm
		-5.79E-02	7621mm - 8000mm
	59.1	-2.66E-02	0mm - 556mm
		2.85E-03	556mm - 6219mm
		1.69E-02	6219mm - 7621mm
		-1.13E-01	7621mm - 8000mm

Hollow core slabs subjected to concentrated loading at the edge can experience longitudinal cracks in the top flange over the unfilled void behind the load due to high tensile stresses. The hollow core slab is constructed with only longitudinal reinforcement, so transverse capacity depends solely on the concrete tensile capacity. Further, it is specified in the hollow core standard NS-EN 1168 that the hollow core slab system can be expected to distribute loads in the system.

The load distribution and tensile stress analysis was done using a finite element analysis tool, Abaqus. First the theory of load distribution in a system of hollow core slabs was analysed, then the results was applied to a single hollow core slab under a concentrated load equal to the weight of two chosen balconies and their respective live loads. The analysis was done with three different slab types HD200, HD265, HD320 and the load was applied to the center of the span, close to the support and at both places. Then the tensile stresses are obtained by varying the vertical and horizontal load, the placement of the connection, the amount of prestress reinforcement, the mesh size and the placement of the connection plate.

The smallest slab type HD200 experience tensile stresses higher than the tensile capacity of the concrete for all the loads presented. HD265 and HD320 experience lower stresses but some are close to the tensile limit. For all the slabs, the worst tensile stresses occur when loaded close to the supports. Moment transferred to the HCS from the balcony is a big influence on the tensile stresses, but they are often not transferred to the hollow core slab due to the connection detail. Other parameters such as placement of the steel plate, amount of prestress reinforcement and the horizontal load in the connection have small influence. Results show that the tensile stresses are mostly affected by the vertical load and the load placement and can cause cracks and failure in the loaded hollow core slab if not designed with caution.

NTNU

Norwegian University of
Science and Technology